

Dyonic Non-Abelian Black Holes

Yves Brihaye¹, Betti Hartmann², Jutta Kunz² and Nadège Tell¹

¹ Faculté des Sciences, Université de Mons-Hainaut
B-7000 Mons, Belgium

²Fachbereich Physik, Universität Oldenburg, Postfach 2503
D-26111 Oldenburg, Germany

March 2, 2018

Abstract

We study static spherically symmetric dyonic black holes in Einstein-Yang-Mills-Higgs theory. As for the magnetic non-abelian black holes, the domain of existence of the dyonic non-abelian black holes is limited with respect to the horizon radius and the dimensionless coupling constant α , which is proportional to the ratio of vector meson mass and Planck mass. At a certain critical value of this coupling constant, $\hat{\alpha}$, the maximal horizon radius is attained. We derive analytically a relation between $\hat{\alpha}$ and the charge of the black hole solutions and confirm this relation numerically. Besides the fundamental dyonic non-abelian black holes, we study radially excited dyonic non-abelian black holes and globally regular gravitating dyons.

Preprint hep-th/9904065

1 Introduction

SU(2) Yang-Mills-Higgs (YMH) theory, with the Higgs field in the adjoint representation, possesses globally regular particle-like solutions, such as the 't Hooft-Polyakov magnetic monopole [1] and the Julia-Zee dyon, which carries both magnetic and electric charge [2].

In SU(2) Einstein-Yang-Mills-Higgs (EYMH) theory, for small gravitational constant the gravitating fundamental monopole [3, 4, 5] and the gravitating fundamental dyon [6] emerge smoothly from the corresponding flat space solutions. The mass of the gravitating fundamental monopole [4, 5] and dyon [6] solutions decreases with increasing gravitational constant, corresponding to increasing coupling constant α , which is proportional to the ratio of vector meson mass and Planck mass. The regular solutions cease to exist beyond some maximal value of α , depending on the electric charge Q [4, 5, 6, 7].

Besides these globally regular solutions, in SU(2) EYMH theory magnetic [4, 5, 8, 9] and dyonic [6] non-abelian black hole solutions exist. They emerge from the globally regular solutions, when a finite regular event horizon x_h is imposed. Consequently, they have been characterized as “black holes within magnetic monopoles” [4] or “black holes within dyons” [6]. Distinct from the corresponding embedded Reissner-Nordström (RN) black holes [10], these non-abelian black hole solutions represent counterexamples to the “no-hair” conjecture, because they carry non-trivial non-Coulomb-like fields outside their horizon. In contrast, pure SU(2) EYM theory possesses neither regular dyon solutions [11], nor dyonic black holes other than embedded RN solutions [12, 13].

The magnetic non-abelian black holes exist only in a limited domain of the $\alpha - x_h$ plane [4, 5, 8]. The domain of existence consists of two regimes, where for fixed coupling constant α and varying horizon radius x_h , the solutions approach limiting solutions in two distinct ways. At the transition point between these two regimes, given by the critical value $\hat{\alpha}$, the maximal horizon radius is attained [5, 8]. Limiting our investigations to vanishing Higgs self-coupling, we here determine the domain of existence of the dyonic non-abelian black holes, finding also two regimes for the coupling constant α .

Besides the fundamental gravitating monopole and dyon solutions there are radially excited solutions [5, 8, 6], where the gauge field function possesses nodes. Both the radially excited monopole and dyon solutions are related to the globally regular Einstein-Yang-Mills (EYM) solutions, found by Bartnik and McKinnon [14], and, like these solutions, have no flat space counterparts. Besides the radially excited globally regular dyon solutions, we here consider the radially excited dyonic non-abelian black hole solutions and determine their domain of existence.

In section II we derive the EYMH equations of motion. We present the equations both in Schwarzschild-like coordinates, employed in the numerical calculations [6], and

in isotropic coordinates, to extend the analytical calculations [8] to the dyonic case. In section III we briefly review the embedded RN solutions. We discuss the globally regular dyon solutions in section IV. In addition to vanishing Higgs self-coupling, we consider the fundamental solutions also for finite Higgs self-coupling, in order to demonstrate that, as in flat space [15], a maximally possible charge Q_{\max} arises. In section V we discuss the dyonic non-abelian black hole solutions. In particular, we derive the critical value $\hat{\alpha}$ for the dyonic solutions analytically and confirm it numerically. For vanishing Higgs self-coupling, we determine the domain of existence for the fundamental and the first radially excited dyonic non-abelian black hole solutions, and we discuss the pattern how the black hole solutions approach limiting solutions. We conclude in section VI. In Appendix A, finally we show the local existence of the non-abelian regular dyon and dyonic black hole solutions at the origin and at the horizon, respectively.

2 Einstein-Yang-Mills-Higgs Equations of Motion

We consider the SU(2) EYMH action

$$S = S_G + S_M = \int L_G \sqrt{-g} d^4x + \int L_M \sqrt{-g} d^4x \quad (1)$$

with

$$L_G = \frac{1}{16\pi G} \mathcal{R} , \quad (2)$$

and

$$L_M = -\frac{1}{4} F_{\mu\nu}^a F^{a\mu\nu} - \frac{1}{2} D_\mu \phi^a D^\mu \phi^a - \frac{\beta^2 g^2}{4} (\phi^a \phi^a - v^2)^2 , \quad (3)$$

where

$$F_{\mu\nu}^a = \partial_\mu A_\nu^a - \partial_\nu A_\mu^a + g \epsilon^{abc} A_\mu^b A_\nu^c , \quad (4)$$

$$D_\mu \phi^a = \partial_\mu \phi^a + g \epsilon^{abc} A_\mu^b \phi^c , \quad (5)$$

g is the gauge coupling constant, β is the dimensionless Higgs coupling constant, proportional to the ratio of Higgs boson mass and vector boson mass, and v is the Higgs field vacuum expectation value. Variation of the action eq. (1) with respect to the metric $g_{\mu\nu}$, the gauge field A_μ^a and the Higgs field ϕ^a leads to the Einstein equations and the matter field equations.

2.1 Ansatz

For static spherically symmetric globally regular and black hole solutions the metric can be parametrized as [8, 16]

$$ds^2 = g_{\mu\nu} dx^\mu dx^\nu = -e^{2\nu(R)} dt^2 + e^{2\lambda(R)} dR^2 + r^2(R) (d\theta^2 + \sin^2 \theta d\phi^2) . \quad (6)$$

For the gauge and Higgs field we employ the spherically symmetric ansatz [6]

$$\vec{A}_t = \vec{e}_r J(r) v , \quad (7)$$

$$\vec{A}_r = 0 , \quad \vec{A}_\theta = -\vec{e}_\phi \frac{1 - K(r)}{g} , \quad \vec{A}_\phi = \vec{e}_\theta \frac{1 - K(r)}{g} \sin \theta , \quad (8)$$

and

$$\vec{\phi} = \vec{e}_r H(r) v , \quad (9)$$

with the standard unit vectors \vec{e}_r , \vec{e}_θ and \vec{e}_ϕ . For $A_t^a = 0$, the solutions carry only magnetic charge [4, 5, 9].

With these ansätze we obtain the action

$$\begin{aligned} S = \frac{1}{G} \int dt dR e^{\nu+\lambda} & \left(\frac{1}{2} \left[1 + e^{-2\lambda} \left((r')^2 + \nu'(r^2)' \right) \right] \right. \\ & + 4\pi G \left[e^{-2(\lambda+\nu)} \frac{r^2}{2} (J')^2 v^2 + e^{-2\nu} K^2 J^2 v^2 \right. \\ & \left. \left. - e^{-2\lambda} \left(\frac{(K')^2}{g^2} + \frac{r^2}{2} (H')^2 v^2 \right) - V_2 \right] \right) , \quad (10) \end{aligned}$$

where ν , λ , r , K , J and H are functions of R , the prime indicates the derivative with respect to R , and

$$V_2 = \frac{(1 - K^2)^2}{2g^2 r^2} + K^2 H^2 v^2 + \frac{\beta^2 g^2}{4} r^2 (H^2 - 1)^2 v^4 . \quad (11)$$

2.2 Schwarzschild-like coordinates

We first employ Schwarzschild-like coordinates, corresponding to the gauge $r(R) = R$. Renaming $R = r$, the spherically symmetric metric reads

$$ds^2 = -A^2 N dt^2 + N^{-1} dr^2 + r^2 (d\theta^2 + \sin^2 \theta d\phi^2) , \quad (12)$$

with the metric functions

$$A(r) = e^{\lambda+\nu} , \quad (13)$$

$$N(r) = 1 - \frac{2m(r)}{r} = e^{-2\lambda} , \quad (14)$$

and the mass function $m(r)$.

We now introduce the dimensionless coordinate x and the dimensionless mass function μ ,

$$x = gvr , \quad \mu = gvm , \quad (15)$$

as well as the dimensionless coupling constant α

$$\alpha^2 = 4\pi Gv^2 . \quad (16)$$

The tt and rr components of the Einstein equations then yield the equations for the metric functions,

$$\begin{aligned} \mu' = \alpha^2 & \left(\frac{x^2 J'^2}{2A^2} + \frac{J^2 K^2}{A^2 N} + NK'^2 + \frac{1}{2} N x^2 H'^2 \right. \\ & \left. + \frac{(K^2 - 1)^2}{2x^2} + H^2 K^2 + \frac{\beta^2}{4} x^2 (H^2 - 1)^2 \right) , \end{aligned} \quad (17)$$

and

$$A' = \alpha^2 x \left(\frac{2J^2 K^2}{A^2 N^2 x^2} + \frac{2K'^2}{x^2} + H'^2 \right) A , \quad (18)$$

where the prime now indicates the derivative with respect to x . For the matter functions we obtain the equations

$$(ANK')' = AK \left(\frac{K^2 - 1}{x^2} + H^2 - \frac{J^2}{A^2 N} \right) , \quad (19)$$

$$\left(\frac{x^2 J'}{A} \right)' = \frac{2JK^2}{AN} , \quad (20)$$

and

$$(x^2 ANH')' = AH (2K^2 + \beta^2 x^2 (H^2 - 1)) . \quad (21)$$

Introducing the new function

$$P = \frac{J}{A} \quad (22)$$

and using eq. (18), we see that the metric function A can be eliminated from the set of equations (17), (19)-(21). These can then be solved separately, with the metric function A being determined subsequently by (18).

In the following we refer to the above set of functions, variables and parameters, also employed in [6], as notation I.

2.3 Isotropic coordinates

To make contact with the analytical results of [5, 8] and to extend them to the case of gravitating dyons and dyonic black holes, we now present the equations of motion

in the notation of [8], in the following referred to as notation II. In the Schwarzschild gauge the following identifications hold

$$\begin{aligned} [6] : & \quad x \quad A \quad N \quad K \quad H \quad J \quad \alpha \quad \beta^2 \\ [8] : & \quad \alpha r \quad e^{\lambda+\nu} \quad e^{-2\lambda} \quad W \quad \alpha H \quad J \quad \alpha \quad \frac{\beta^2}{2} \end{aligned} \quad (23)$$

Along with [8], we now employ the gauge choice $e^\lambda = \frac{r(R)}{R}$, corresponding to isotropic coordinates, and introduce the coordinate

$$\tau = \ln R, \quad (24)$$

and the dot ($\dot{}$) now indicates the derivative with respect to τ . To obtain a system of first order equations we further employ for the first derivatives the new variables [8]

$$N = \frac{\dot{r}}{r}, \quad \kappa = \dot{\nu} + N, \quad U = \frac{\dot{W}}{r}, \quad V = \dot{H}, \quad (25)$$

and we introduce

$$B = e^{-\nu} J, \quad C = \dot{B}. \quad (26)$$

(Note, that the symbol N here has a totally different meaning from eq. (14).)

Then the following system of first order autonomous equations is obtained

$$\dot{r} = Nr \quad (27)$$

$$\dot{N} = N(\kappa - N) - (2U^2 + V^2) - 2\alpha^2 B^2 W^2 \quad (28)$$

$$\dot{\kappa} = 1 - \kappa^2 + 2U^2 - \frac{\beta^2 r^2}{2} (H^2 - \alpha^2)^2 - 2W^2 H^2 + 2\alpha^2 W^2 B^2 \quad (29)$$

$$\dot{H} = V \quad (30)$$

$$\dot{V} = \frac{\beta^2 r^2}{2} (H^2 - \alpha^2) H + 2W^2 H - \kappa V \quad (31)$$

$$\dot{W} = rU \quad (32)$$

$$\dot{U} = U(N - \kappa) + \frac{W(W^2 - 1)}{r} + W r (H^2 - \alpha^2 B^2) \quad (33)$$

$$\dot{B} = C \quad (34)$$

$$\begin{aligned} \dot{C} = & \quad -\kappa C + B(2W^2 - 4U^2 - V^2 + \kappa^2 - 1 \\ & \quad + 2W^2 H^2 + \frac{\beta^2 r^2}{2} (H^2 - \alpha^2)^2) - 4\alpha^2 B^3 W^2 \end{aligned} \quad (35)$$

supplemented by the constraint

$$2\kappa N = 1 + N^2 + 2U^2 + V^2 - 2V_2 + 2\alpha^2 W^2 B^2 - \alpha^2 (C + B(\kappa - N))^2 \quad (36)$$

compatible with the equations.

3 Embedded Reissner-Nordström Solutions

As noted long ago [10], the Einstein-Yang-Mills-Higgs system admits embedded RN solutions. In notation I, RN solutions with mass μ_∞ , unit magnetic charge and arbitrary electric charge Q are given by

$$\mu(x) = \mu_\infty - \frac{\alpha^2(1+Q^2)}{2x}, \quad A(x) = 1, \quad (37)$$

$$K(x) = 0, \quad J(x) = J_\infty - \frac{Q}{x}, \quad H(x) = 1, \quad (38)$$

where J_∞ is a priori arbitrary, but here chosen as $J_\infty = Q/x_h$ (see eq. (51)). At the regular horizon x_h the metric function

$$N(x) = \frac{x^2 - 2x\mu_\infty + \alpha^2(1+Q^2)}{x^2} \quad (39)$$

vanishes, $N(x_h) = 0$, yielding

$$x_h = \mu_\infty + \sqrt{\mu_\infty^2 - \alpha^2(1+Q^2)} \quad (40)$$

or equivalently

$$\mu_\infty = \frac{x_h^2 + \alpha^2(1+Q^2)}{2x_h}. \quad (41)$$

For fixed values of α and Q , RN solutions exist for $x_h \geq \alpha\sqrt{1+Q^2}$, independent of β .

In the extremal case

$$x_h = \mu_\infty = \alpha\sqrt{1+Q^2}, \quad (42)$$

extremal RN solutions are obtained. Extremal RN solutions are characterized by Q and α . In particular, for extremal RN solutions the function $B(x)$ defined in (26) becomes constant

$$B = \frac{J}{A\sqrt{N}} = \frac{Q}{\alpha\sqrt{1+Q^2}}. \quad (43)$$

4 Dyon Solutions

Let us first consider the globally regular particle-like solutions of the SU(2) EYMH system.

In the Prasad-Sommerfield limit, $\beta = 0$, the dyon solutions in flat space are known analytically [2], whereas for finite β they are obtained only numerically [15]. In the presence of gravity, the corresponding gravitating monopole and dyon solutions are obtained only numerically as well. The gravitating dyon solutions have many features in common with the gravitating monopole solutions [6].

After presenting the boundary conditions for the asymptotically flat globally regular solutions, we here briefly discuss the fundamental dyon solutions both in the Prasad-Sommerfield limit and for finite β . Then we turn to the excited dyon solutions.

4.1 Boundary conditions

Requiring asymptotically flat solutions implies in notation I that the metric functions A and μ both approach a constant at infinity. We here adopt

$$A(\infty) = 1 , \tag{44}$$

and $\mu(\infty) = \mu_\infty$ represents the dimensionless mass of the solutions. The matter functions also approach constants asymptotically,

$$K(\infty) = 0 , \quad J(\infty) = J_\infty , \quad H(\infty) = 1 , \tag{45}$$

where for magnetic monopole solutions $J_\infty = 0$. The asymptotic fall-off of the function $J(x)$ determines the dimensionless electric charge Q (see eq. (38)).

Regularity of the solutions at the origin requires

$$\mu(0) = 0 , \tag{46}$$

and [2]

$$K(0) = 1 , \quad J(0) = 0 , \quad H(0) = 0 . \tag{47}$$

The local existence of a family of analytic solutions obeying these conditions is shown in Appendix A.1.

4.2 Fundamental dyons

$\beta = 0$

Like the gravitating monopole solutions, the gravitating dyon solutions exist up to a maximal value of the coupling constant α . Beyond this value no dyon solutions exist. The fundamental dyon branch does not end at the maximal value α_{\max} , but bends backwards and extends up to the critical value α_c . Since $\alpha^2 = 4\pi Gv^2$, variation of the coupling constant along the fundamental dyon branch can be considered as first increasing G with v fixed up to the maximal value α_{\max} , and then decreasing v with G fixed up to the critical value α_c .

Completely analogously to the fundamental monopole branch [5], the fundamental dyon branch reaches a limiting solution at the critical value α_c , where it bifurcates with the branch of extremal RN solutions of unit magnetic charge and electric charge Q [6]. The critical value $\alpha_c(Q)$ depends only slightly on the charge Q [6].

For $\alpha \rightarrow \alpha_c$ the minimum of the metric function $N(x)$ of the dyon solutions decreases monotonically, approaching zero at $x_c = \alpha_c \sqrt{1 + Q^2}$. For $x \geq x_c$, the metric function $N(x)$ of the limiting solution corresponds to the metric function of the extremal RN black hole with horizon $x_h = x_c = \alpha_c \sqrt{1 + Q^2}$, unit magnetic charge and electric charge Q . Likewise, for $x \geq x_c$, the other functions of the limiting solution correspond to those of this extremal RN black hole [6]. Consequently, also the mass of the limiting solution coincides with the mass of this extremal RN black hole.

On the interval $0 \leq x \leq x_c$ the functions $N(x)$, $K(x)$ and $H(x)$ of the limiting solution vary smoothly from their respective boundary values at $x = 0$ to those of the extremal RN solution at x_c , whereas the function $J(x)$ is identically zero. The metric function $A(x)$ is identically zero, as well, on the interval $0 \leq x < x_c$, but discontinuous at x_c . Consequently, in the limiting spacetime the inner and outer parts are not analytically connected [4, 5].

$\beta > 0$

Let us briefly consider the dyon solutions for finite Higgs self-coupling, $\beta > 0$, because we here encounter a phenomenon, also present for the black hole solutions at vanishing Higgs self-coupling, $\beta = 0$.

In flat space dyon solutions of arbitrarily large charge exist only for $\beta = 0$. In contrast, for finite values of β dyon solutions exist only up to a maximal value of the charge, $Q_{\max}(\beta)$ [15]. As the maximal value of the charge is approached, the function $J(x)$ approaches asymptotically the limiting value

$$\lim_{Q \rightarrow Q_{\max}} J_{\infty} = 1 . \quad (48)$$

At this point the solutions change character and become oscillating instead of asymptotically decaying [15].

As illustrated in Figs. 1-2, this phenomenon persists in curved space. In Fig. 1 we show the mass of the flat space dyon (solid line) and of the gravitating dyon (dashed line, corresponding to $\alpha = 0.5$) as a function of the charge Q for $\beta^2 = 0$ and $\beta^2 = 0.5$. In Fig. 2 the corresponding asymptotic values of the function $J(x)$ are presented. We note, that for finite β also gravitating dyon solutions exist only up to a maximal value of the charge, where $J_{\infty} \rightarrow 1$.

4.3 Radially excited dyons

Besides the branch of fundamental dyon solutions there are branches of radially excited dyon solutions, where the gauge field function $K(x)$ of the n -th radially excited dyon solution has n nodes.

These solutions have no flat space counterparts, and the variation of α along a branch of excited solutions must be interpreted as a variation of v with G fixed. In the limit $\alpha \rightarrow 0$ the Higgs field vacuum expectation value therefore vanishes, while G

remains finite. Because of the particular choice of dimensionless variables (15), in this limit the solutions shrink to zero size and their mass μ diverges. As for the radially excited monopole solutions [5], the coordinate transformation $\tilde{x} = x/\alpha$ leads to finite limiting solutions in the limit $\alpha \rightarrow 0$, which are the Bartnik-McKinnon solutions [6].

In Fig. 3 we show the normalized mass μ_∞/α as a function of α for the first excited dyon branch with electric charge $Q = 1$ and $\beta = 0$. For comparison also the first excited monopole branch is shown.

Like the radially excited monopole solutions, the radially excited dyon solutions exist only below a critical value of the coupling constant α . For the radially excited monopole solutions this critical value is $\alpha_c = \sqrt{3}/2$ [5, 8]. For the radially excited dyon solutions the critical value is larger and will be discussed in the context of the dyonic black hole solutions.

5 Black Hole Solutions

We now turn to the dyonic black hole solutions of the SU(2) EYMH system, choosing $\beta = 0$. Again, the SU(2) EYMH dyonic black holes have many features in common with the magnetic non-abelian black holes [6]. In particular, dyonic non-abelian black hole solutions exist in a limited domain of the α - x_h plane, which depends on the charge Q , and, in the limit $x_h \rightarrow 0$, the corresponding globally regular solutions are obtained. But a new phenomenon occurs for small values of α , where the non-abelian solutions no longer bifurcate with non-extremal RN solutions.

In the following, we briefly present the boundary conditions. We generalize the considerations of [8] to dyonic solutions and derive analytically the critical value of the coupling constant, $\hat{\alpha}$. We then present our numerical calculations for the fundamental dyonic black hole solutions and their radial excitations.

5.1 Boundary conditions

Imposing the condition of asymptotic flatness, the black hole solutions satisfy the same boundary conditions at infinity as the regular solutions. The existence of a regular event horizon at x_h leads in notation I to the conditions for the metric functions

$$\mu(x_h) = \frac{x_h}{2}, \quad (49)$$

and $A(x_h) < \infty$, and for the matter functions

$$N'K'|_{x_h} = K \left(\frac{K^2 - 1}{x^2} + H^2 \right) \Big|_{x_h}, \quad (50)$$

$$J|_{x_h} = 0, \quad (51)$$

and

$$x^2 N' H'|_{x_h} = H \left(2K^2 + \beta^2 x^2 (H^2 - 1) \right) \Big|_{x_h} . \quad (52)$$

The local existence of a family of solutions obeying these conditions at the horizon is demonstrated in Appendix A.2.

5.2 Critical value of α

For magnetic black holes, there are two regimes of the coupling constant α , corresponding to two distinct patterns of reaching a limiting solution as a function of the horizon radius x_h . For larger values of α , the solutions bifurcate with an extremal RN black hole solution, when the horizon radius approaches its critical value x_h^{cr} . Here the solutions tend towards the corresponding extremal RN solution with horizon radius $x_h^{\text{RN}} = \alpha$ only on the interval $x \geq x_h^{\text{RN}}$, whereas they tend to a generic non-abelian limiting solution on the interval $x_h^{\text{cr}} \leq x \leq x_h^{\text{RN}}$ [6]. In contrast for smaller values of α the solutions bifurcate with a non-extremal RN solution on the full interval $x \geq x_h^{\text{cr}}$ [5, 8]. The transition point between these two regimes corresponds to the critical value $\hat{\alpha}$, where the non-abelian black hole solutions tend towards the extremal RN solution with horizon radius $x_h^{\text{RN}} = \hat{\alpha}$ on the full interval $x \geq x_h^{\text{cr}} = x_h^{\text{RN}}$, i.e. x_h^{cr} and x_h^{RN} coincide. For the magnetic non-abelian black holes this critical value is given by $\hat{\alpha} = \sqrt{3}/2$ [5, 8].

Analogously, for dyonic non-abelian black holes there are also two regimes of the coupling constant α , with $\hat{\alpha}$ marking the transition point between these two regimes. We now derive this critical value $\hat{\alpha}$ for the dyonic non-abelian black hole solutions, following closely the reasoning of [8].

Let us then consider the fixed points of the system (27)-(35). Employing notation II, the relevant fixed point is given by the configuration

$$H_h = \alpha , \quad W_h = 0 , \quad \kappa_h = 1 , \quad r_h = \frac{1}{\sqrt{1 - \alpha^2 B_h^2}} , \quad (53)$$

where $N_h = V_h = U_h = C_h = 0$, while B_h is such that $0 \leq B_h \leq 1/\alpha$.

Linearization of the equations about this fixed point leads to the following eigenvalues of the matrix defining the linear part (adopting the order $N, W, U, H, V, P, Q, \kappa$)

$$\gamma_0 = 1 \quad (54)$$

$$\gamma_{1,2} = -\frac{1}{2} \pm i \sqrt{\frac{3}{4} - \alpha^2 \frac{1 - B_h^2}{1 - \alpha^2 B_h^2}} \quad (55)$$

$$\gamma_{3,4} = -\frac{1}{2} \pm \sqrt{\frac{1}{4} + \alpha^2 \beta^2 r_h^2} \quad (56)$$

$$\gamma_5 = 0 \quad (57)$$

$$\gamma_6 = -1 \quad (58)$$

$$\gamma_7 = -2 \quad (59)$$

In particular, we see that the eigenvalues $\gamma_{1,2}$, which are related to the function W and determine the critical value $\hat{\alpha}$ for the magnetic black holes [8], now depend on B_h . The zero mode γ_5 is related to the occurrence of this free parameter.

For $Q = 0$, the critical value of α corresponds to the transition of the eigenvalue $\gamma_{1,2}$ (eq. (55) for $Q = 0$) from complex to real value [8]. Repeating this reasoning for dyonic black holes, we conclude, that the corresponding critical value of the coupling constant for the dyonic non-abelian black holes is given by

$$\hat{\alpha}^2 = \frac{3}{4 - B_h^2} . \quad (60)$$

Here the relation of the critical value $\hat{\alpha}$ to the charge Q seems only indirect, since the value of the function $B(x)$ at the horizon enters in eq. (60). However, for the dyonic non-abelian black holes $\hat{\alpha}$ also represents the special point, where the non-abelian black hole solutions tend towards the corresponding extremal RN solution with horizon radius $x_h^{\text{RN}} = \hat{\alpha} \sqrt{1 + Q^2}$ on the full interval $x \geq x_h^{\text{cr}} = x_h^{\text{RN}}$. This implies for the function $B(x)$ according to eq. (43)

$$\lim_{\alpha \rightarrow \hat{\alpha}} B(x) = \frac{Q}{\hat{\alpha} \sqrt{1 + Q^2}} , \quad \forall x > x_h^{\text{RN}} . \quad (61)$$

Consequently, we may insert for B_h in eq. (60) the constant RN value, eq. (43), and obtain for the critical coupling constant the expression

$$\hat{\alpha}(Q) = \sqrt{\frac{3 + 4Q^2}{4(1 + Q^2)}} , \quad (62)$$

which now depends on the electric charge Q .

5.3 Fundamental dyonic black holes

Let us now define some quantities helpful in the analysis of the numerical results. Denoting the set of functions of the extremal RN solution with horizon radius $x_h^{\text{RN}} = \alpha \sqrt{1 + Q^2}$ by $(N_{\text{RN}}, K_{\text{RN}}, H_{\text{RN}}, P_{\text{RN}})$, and denoting the set of functions of the non-abelian black hole solution with horizon radius x_h (with $x_h < x_h^{\text{RN}}$) by (N, K, H, P) , we define

$$DN = \max_{x \in [x_h^{\text{RN}}, \infty]} |N_{\text{RN}}(x) - N(x)| , \quad (63)$$

and analogously we define the quantities DK , DP and DH . Clearly the quantities DN , DK , DP and DH must vanish, when the non-abelian black hole solutions bifurcate with the corresponding extremal RN solution. Therefore these quantities help to determine the critical values with good accuracy in the regime $\alpha \geq \hat{\alpha}$.

$Q = 0$

Our numerical evaluation of the domain of existence of the magnetic non-abelian black holes in the α - x_h plane is in agreement with the results of [5, 8], and in particular we confirm $\hat{\alpha} = \sqrt{3}/2$. Considering the quantities DN , DK and DH (eq. (63)) as functions of the horizon radius x_h , we observe that for $\alpha \geq \hat{\alpha}$ the three functions approach zero at a common value $x_h^{\text{cr}}(\alpha) \leq \hat{\alpha}$. As $\alpha - \hat{\alpha}$ changes sign, in particular the quantity DK changes drastically, becoming a convex function when the critical horizon radius x_h^{cr} is approached.

$Q \neq 0$

We have numerically determined the domain of existence of the fundamental dyonic non-abelian black hole solutions in the α - x_h plane, which is shown in Fig. 4 for $Q = 1$. The straight line indicates the extremal RN solutions, dividing the domain of existence into a lower region with non-abelian black holes only and an upper region with both non-abelian and non-extremal abelian black holes, completely analogously to the case of magnetic black holes.

To start the detailed discussion of the diagram, we choose a small fixed value of the horizon radius x_h and vary α . Then the dyonic black hole solutions exist only up to some maximal value $\alpha_{\text{max}}(x_h)$. From $\alpha_{\text{max}}(x_h)$ a second branch extends backwards until a critical value $\alpha_c(x_h)$ is reached. With increasing x_h the second branch becomes increasingly smaller, and finally disappears. The critical values $\alpha_{\text{max}}(x_h)$ and $\alpha_c(x_h)$ are both shown in Fig. 4.

The presence of the two branches is illustrated in Fig. 5 for $Q = 1$ and $x_h = 0.8$, where the quantities DN , DK , DP and DH are shown as functions of the parameter α . Here the second branch of solutions only exists in the small interval $1.1986 \leq \alpha \leq 1.2002$.

For fixed x_h and varying α , the functions of the black holes solutions evolve completely analogously to those of the regular dyon solutions. Consequently, the limiting solution reached at the critical value $\alpha_c(x_h)$ consists of two parts, the outer part corresponding to the exterior of the extremal RN black hole with horizon $x_h^{\text{RN}} = \alpha_c \sqrt{1 + Q^2}$, unit magnetic charge and electric charge Q and the inner part representing a genuine non-abelian solution.

Similarly for fixed $\alpha > \hat{\alpha}$ and varying x_h , the limiting solution reached consists of two parts, the outer part corresponding to the exterior of the extremal RN black hole with horizon $x_h^{\text{RN}} = \alpha \sqrt{1 + Q^2}$, unit magnetic charge and electric charge Q , as demonstrated in Figs. 6-7 for the black hole solutions with horizon $x_h = 1, 1.1$ and 1.153 , charge $Q = 1$ and $\alpha = 1$ for the functions N and P and the functions K and H ,

respectively.

According to eq. (62), for $Q = 1$ the critical value $\hat{\alpha}$ is given by $\hat{\alpha} = \sqrt{7/8} \approx 0.935$. Here the transition between the two regimes with different bifurcation patterns is supposed to occur. Indeed, our numerical calculations confirm this critical value, as demonstrated in Figs. 8-9, where the four quantities DN , DK , DP and DH are shown as functions of the horizon radius x_h for $\alpha = 0.94$ and $\alpha = 0.93$, respectively.

For $\alpha = 0.94$, which is slightly above $\hat{\alpha}$, the curves in Fig. 8 clearly approach zero at $x_h^{\text{cr}} \approx 1.235$. This value is well below the horizon value of the corresponding extremal RN solution, $x_h^{\text{RN}} = \alpha\sqrt{1+Q^2} \approx 1.329$. Moreover, in this limit $x_h \rightarrow x_h^{\text{cr}}$, the corresponding values of $K(x_h)$ and $H(x_h)$ do not tend to their RN values of zero and one, respectively, but they converge to generic numbers in the interval $[0, 1]$.

In contrast, for $\alpha = 0.93$, which is slightly below $\hat{\alpha}$, the function DK becomes a convex function when the critical horizon radius $x_h^{\text{cr}} \approx 0.93\sqrt{2} \approx 1.315$ is approached. Furthermore, the quantities $K(x_h)$ and $H(x_h)$ tend to their RN values zero and one, respectively, for $x_h \rightarrow x_h^{\text{cr}}$. Thus for $\alpha = 0.93$ the limiting solution represents a RN solution on the full interval $x \geq x_h^{\text{cr}}$.

Clearly, the transition point $\hat{\alpha}$ occurs inbetween these two values. Approaching $\hat{\alpha}$ further from both sides, the value $\hat{\alpha} = \sqrt{7/8} \approx 0.935$ is confirmed. The gap in Fig. 4 on the rhs of $\hat{\alpha}$ represents a tiny region, numerically not accessible with sufficient accuracy [17]. We have confirmed the validity of eq. (62) also for other values of the charge Q .

In the regime $\alpha < \hat{\alpha}$, we observe that the maximal value of the horizon radius x_h decreases with decreasing α , completely analogously to the magnetic case. Continuing our detailed discussion of the approach to the limiting solution in this regime, however, we observe differences to the magnetic case for smaller values of α and larger values of Q .

For fixed α close to $\hat{\alpha}$ and increasing x_h , the dyonic black hole solutions bifurcate with a RN solution when the maximal value of the horizon is reached. The limiting solution corresponds to the exterior of the RN solution on the full interval $x \geq x_h^{\text{cr}}$. For smaller values of Q and somewhat smaller fixed α , with increasing x_h the solutions do not yet bifurcate with a non-extremal RN solution, when the maximal value of the horizon is reached. Instead a second branch of solutions emerges, extending backwards to lower values of the horizon radius, until it bifurcates with a non-extremal RN solution at the critical value of the horizon x_h^{cr} [5, 8, 6]. Moving along both branches, the values of $K(x_h)$ and $H(x_h)$ change monotonically, reaching their respective RN values of zero and one as the critical horizon is reached.

For the magnetic black holes as well as for the dyonic black holes with smaller values of Q this latter bifurcation pattern persists with decreasing α [5, 8]. In contrast, for the dyonic non-abelian black holes with larger values of Q new phenomena occur.

We exhibit these new phenomena in Fig. 10, where the critical region of the α - x_h plane shown in Fig. 4 for $Q = 1$ is enlarged and more details are given. First, we

observe the occurrence of bifurcations, which lead to the small triangular region ABC , where three solutions exist. Thus below $\hat{\alpha}$ we find four distinct regions in the α - x_h plane. With decreasing α and increasing x_h there are i) for $0.605 < \alpha$ first one, then zero solutions, ii) for $0.575 < \alpha < 0.605$ first one, then three, then one, then zero solutions, iii) for $0.535 < \alpha < 0.575$ first one, then three, then two, then zero solutions and iv) for $\alpha < 0.535$ first one, then two, then zero solutions.

Second, with decreasing α , the value J_∞ of the limiting solution increases. When it reaches its maximal value of one, the function $K(x)$ ceases to decay exponentially. The limiting solution then no longer represents a non-extremal RN solution, instead an oscillating solution is reached as the limiting solution. The corresponding critical point, where the transition from the limiting non-extremal RN solutions to the oscillating solutions occurs, is labelled D in Fig. 10. Along the curve BD the maximal value of the horizon radius is reached when the limiting value $J_\infty = 1$ is attained, whereas along the curves AB and $A'A$ an intermediate extremal value of the horizon radius is reached when the limiting value $J_\infty = 1$ is attained.

Figs. 11-13 illustrate both phenomena, representing the values $K(x_h)$, $H(x_h)$ and J_∞ as functions of the horizon radius for $\alpha = 0.7$, 0.55 and 0.2 , respectively. As seen in Fig. 11, for $\alpha = 0.7$ only one branch of solutions exists. Here, with increasing x_h $K(x_h)$ decreases monotonically to zero, $H(x_h)$ increases monotonically to one, while J_∞ increases monotonically to a limiting value smaller than one. Decreasing α , the critical point C of Fig. 10 is reached, below which three branches of solutions exist. Moving along the three branches, $K(x_h)$ decreases monotonically, $H(x_h)$ increases monotonically and J_∞ increases monotonically until it reaches one, as seen in Fig. 12 for $\alpha = 0.55$. For still smaller values of α , at the critical value A , the third branch disappears, leaving two branches which end when J_∞ reaches one. This is seen in Fig. 13 for $\alpha = 0.2$. The maximal horizon radius in this case is approximately 0.917 . For small values of α (i.e. below the critical point A) the lower curve in Fig. 4 represents the critical value of the horizon, where the asymptotically exponentially decaying solutions cease to exist.

Considering the Q -dependence of the new phenomena, we observe that the bifurcations leading to three branches arise only for $Q \geq 0.8$, and the limiting value $J_\infty = 1$ is reached only for $Q \geq 0.75$. The latter is seen in Fig. 14, where the critical value D is shown, which marks the transition from the limiting non-extremal RN solutions to the oscillating solutions. Also shown in Fig. 14 is the critical value $\hat{\alpha}$. We note, that with increasing Q the two curves get increasingly closer.

5.4 Excited dyonic black holes

Besides the fundamental magnetic black hole solutions there exist radially excited black hole solutions, for which the gauge function $K(x)$ possesses n nodes [5, 8]. These radially excited solutions exist only for $\alpha \leq \hat{\alpha} = \sqrt{3}/2$ [5, 8].

Our numerical analysis of the radially excited dyonic black hole solutions strongly indicates that, at least for $n = 1$, the excited dyonic black hole solutions penetrate into a small domain of the $\alpha > \hat{\alpha}$ regime, as can already be anticipated from Fig. 3, where the first excited regular dyon solution is shown for charge $Q = 1$. Indeed, we observe that the maximal value of α , where the radially excited black hole solutions cease to exist, increases more strongly with Q than the critical value $\hat{\alpha}$.

Let us now consider the domain of existence of the black hole solutions in the $\alpha - x_h$ plane in more detail. In the regime $\alpha > \hat{\alpha}$, for fixed x_h and increasing α the solutions again reach a limiting solution at the critical value $\alpha_c(x_h)$, which consists of two parts, the outer part corresponding to the exterior of the extremal RN black hole with horizon $x_h^{\text{RN}} = \alpha_c \sqrt{1 + Q^2}$, unit magnetic charge and electric charge Q .

For $\alpha \rightarrow \alpha_c(x_h)$ the function $N(x)$ develops a progressively decreasing minimum, N_{min} , reaching zero at $x_h^{\text{RN}} = \alpha_c(x_h) \sqrt{1 + Q^2}$. This is illustrated in Fig. 15, where the value of N_{min} is shown as a function of α for the horizon radii $x_h = 0.01, 0.4$ and 0.8 and charge $Q = 1$. With increasing x_h the value of $\alpha_c(x_h)$ decreases, though it remains greater than $\hat{\alpha}$ even for $x_h = 0.8$, as inspection of the four quantities DN , DK , DP and DH reveals.

In Fig. 16 we show the functions $N(x)$, $K(x)$, $H(x)$ and $P(x)$ of the first radially excited black hole solution for charge $Q = 1$, horizon radius $x_h = 0.4$ and $\alpha = 0.938 > \hat{\alpha}$. The minimum of the function $N(x)$, which here occurs close to $x_h^{\text{RN}} = \alpha_c(x_h) \sqrt{1 + Q^2}$, remains well separated from the horizon x_h for $\alpha \rightarrow \alpha_c(x_h)$.

Considering finally the first excited black hole solutions for small fixed α and increasing x_h , we observe that as for the fundamental black hole solutions, the quantity J_∞ here plays a major role. With increasing x_h , J_∞ approaches its maximal value one, where the asymptotically exponentially decaying solutions cease to exist. For $\alpha = 0.2$, for instance, this happens at $x_h \approx 0.28$.

6 Conclusions

In analogy to gravitating monopoles [4, 5, 7] also gravitating dyons [6] exist. When a regular horizon x_h is imposed, from these solutions “black holes within monopoles” [4, 5] and “black holes within dyons” [6] emerge. Besides the fundamental regular and black hole solutions also radially excited solutions exist [5, 8, 6], related to the corresponding EYM solutions [14, 18]. The static spherically symmetric “black holes within monopoles” and “black holes within dyons” provide counterexamples to the “no-hair conjecture”.

The domain of existence of the fundamental dyonic non-abelian black hole solutions in the $\alpha - x_h$ plane is similar to the one of the fundamental magnetic non-abelian black hole solutions. There are two regimes of the coupling constant α . For $\alpha < \hat{\alpha}$, the maximal horizon radius increases with increasing α , whereas for $\alpha > \hat{\alpha}$ it decreases.

The transition point between these two regimes, $\hat{\alpha}$, depends on the charge Q of the solutions, $\hat{\alpha} = \sqrt{(3 + 4Q^2)/(4(1 + Q^2))}$.

For fixed α and varying horizon radius, a limiting solution is approached. For $\alpha > \hat{\alpha}$ the limiting solution consists of two distinct parts. The outer part corresponds to the exterior of an extremal RN black hole solution with horizon radius $x_h^{\text{RN}} = \alpha\sqrt{1 + Q^2}$, unit magnetic charge and electric charge Q , whereas on the interval $x_h \leq x < x_h^{\text{RN}}$ the limiting solution has the features of generic non-abelian solutions. At the transition point $\alpha = \hat{\alpha}$ the limiting solution corresponds precisely to the exterior of the extremal RN black hole solution with horizon radius $x_h^{\text{RN}} = \hat{\alpha}\sqrt{1 + Q^2}$, on the full interval $x \geq x_h$. In contrast, for $\alpha < \hat{\alpha}$ the limiting solution represents the exterior of a non-extremal RN solution for the larger values of α , while for the smaller values of α the dyonic non-abelian black hole solutions encounter a critical point, where the solutions no longer are exponentially decaying but become oscillating.

The domain of existence of the radially excited dyonic non-abelian black hole solutions in the $\alpha - x_h$ plane is similar to the one of the fundamental solutions. Again, there are two regimes of the coupling constant α with the transition point $\hat{\alpha}$. This is in contrast to the radially excited magnetic non-abelian black hole solutions, which exist only up to $\hat{\alpha}$ [5, 8].

In a large part of their domain of existence, the magnetic non-abelian black hole solutions are classically stable [4, 5, 8, 19]. In contrast, dyonic non-abelian black hole solutions should be classically unstable. As for the classical dyon solutions in flat space, their mass should be lowered continuously, by lowering the electric charge, as long as there is no charge quantization [2].

References

- [1] G. 't Hooft, Nucl. Phys. B79 (1974) 276;
A.M. Polyakov, JETP Lett. 20 (1974) 194.
- [2] Poles with both magnetic and electric charges in non-Abelian gauge theory, Phys. Rev. D11 (1975) 2227;
M.K. Prasad and C.M. Sommerfield, Exact classical solution for the 't Hooft Monopole and the Julia-Zee dyon, Phys. Rev. Lett. 35 (1975) 760.
- [3] P. van Nieuwenhuizen, D.Wilkinson and M.J.Perry, Phys. Rev. D13 (1976) 778.
- [4] K. Lee, V.P. Nair and E.J. Weinberg, Black holes in magnetic monopoles, Phys. Rev. D45 (1992) 2751.
- [5] P. Breitenlohner, P. Forgacs and D. Maison, Gravitating monopole solutions, Nucl. Phys. B383 (1992) 357.

- [6] Y. Brihaye, B. Hartmann, J. Kunz, Gravitating dyons and dyonic black holes, Phys. Lett. B441 (1998) 77.
- [7] A. Lue and E.J. Weinberg, Magnetic monopoles near the black hole threshold, preprint hep-th/9905223.
- [8] P. Breitenlohner, P. Forgacs and D. Maison, Gravitating monopole solutions II, Nucl. Phys. B442 (1995) 126.
- [9] P.C. Aichelburg and P. Bizon, Magnetically charged black holes and their stability, Phys. Rev. D48 (1993) 607.
- [10] F.A. Bais and R.J. Russell, Phys. Rev. D11 (1975) 2692;
Y.M. Cho and P.G.O. Freund, Phys. Rev. D12 (1975) 1588.
- [11] A.A. Ershov and D.V. Gal'tsov, Phys. Lett. 150A (1990) 159.
- [12] D.V. Gal'tsov and A.A. Ershov, Non-abelian baldness of colored black holes, Phys. Lett. A138 (1989) 160.
- [13] P. Bizon and O.T. Popp, No-hair theorem for spherical monopoles and dyons in SU(2) Einstein-Yang-Mills theory, Class. Quantum Grav. 9 (1992) 193.
- [14] R. Bartnik, and J. McKinnon, Particlelike solutions of the Einstein-Yang-Mills equations, Phys. Rev. Lett. 61 (1988) 141.
- [15] Y. Brihaye, B. Kleihaus and D.H. Tchrakian, Dyon-Skyrmion lumps, preprint hep-th/9805059.
- [16] P. G. Bergmann, M. Cahen and A. B. Komar, J. Math. Phys. 6 (1965) 1.
- [17] For the magnetic non-abelian black holes a gap occurs at $\hat{\alpha}$ [8].
- [18] M.S. Volkov, and D.V. Gal'tsov, Black holes in Einstein-Yang-Mills theory, Sov. J. Nucl. Phys. 51 (1990) 747;
P. Bizon, Colored black holes, Phys. Rev. Lett. 64 (1990) 2844;
H. P. Künzle and A. K. M. Masoud-ul-Alam, Spherically symmetric static SU(2) Einstein-Yang-Mills fields, J. Math. Phys. 31 (1990) 928.
- [19] H. Hollmann, On the Stability of Gravitating Nonabelian Monopoles, Phys. Lett. B338 (1994) 181.

7 Appendix A

We show the local existence of the non-abelian dyon solutions at the singular point $x = 0$ in Appendix A.1 and the local existence of the non-abelian dyonic black hole solutions at the singular point x_h in Appendix A.2.

7.1 Appendix A.1

As for the monopoles, the field equations for the dyons have singular points at $x = 0$ and $x = \infty$. For the monopoles there exists a two-parameter family of local solutions regular at $x = 0$. Analogously, for the dyons there exists a three-parameter family of local solutions regular at $x = 0$, as shown in the following.

Let us consider eqs. (17)-(21), using notation I. At the singular point $x = 0$, the expansion of regular solutions depends on four parameters, yielding

$$\begin{aligned}
 N(x) &= 1 - n_2 x^2 + O(x^4) , \\
 A(x) &= A_0(1 + a_2 x^2 + O(x^4)) , \\
 K(x) &= 1 - k_2 x^2 + O(x^4) , \\
 J(x) &= A_0(j_1 x + O(x^3)) , \\
 H(x) &= h_1 x + O(x^3) ,
 \end{aligned} \tag{64}$$

where A_0 , h_1 , j_1 and k_2 are arbitrary parameters while

$$\begin{aligned}
 a_2 &= \alpha^2(j_1^2 + 4k_2^2 + \frac{h_1^2}{2}) , \\
 n_2 &= \alpha^2(j_1^2 + h_1^2 + 4k_2^2 + \frac{\beta^2}{6}) .
 \end{aligned} \tag{65}$$

Eliminating the metric function A , we now show that the remaining equations for N , K , H and P admit a three-parameter family of local solutions near $x = 0$, analytic in the parameters. This is the counterpart of Proposition 2 of Appendix A of [5] in the presence of the dyon degree of freedom. Let us define

$$\begin{aligned}
 w_1 &= \frac{H}{x} , \quad w_2 = NH' , \quad w_3 = \frac{1 - K}{x^2} , \quad w_4 = \frac{NK'}{x} , \\
 w_5 &= \frac{P}{x} , \quad w_6 = (P' + PM)N , \quad w_7 = \frac{1 - N}{x^2}
 \end{aligned} \tag{66}$$

with

$$M = \frac{A'}{A} = \alpha^2 x \left(\frac{2P^2 K^2}{N^2 x^2} + \frac{2K'^2}{x^2} + H'^2 \right) \tag{67}$$

and furthermore

$$\begin{aligned}
u_1 &= \frac{1}{3}(2w_1 + w_2) , & u_2 &= \frac{1}{3}(w_3 - w_4) , & u_3 &= \frac{1}{3}(2w_5 + w_6) , \\
v_1 &= \frac{1}{3}(w_1 - w_2) , & v_2 &= \frac{1}{3}(2w_3 + w_4) , & v_3 &= \frac{1}{3}(w_5 - w_6) , \\
v_4 &= \frac{w_7}{2} - \frac{\alpha^2}{2}(u_1^2 - 2v_1^2 + 4u_2^2 - 2v_2^2 + u_3^2 - 2v_3^2 + \frac{\beta^2}{6}) .
\end{aligned} \tag{68}$$

Then eqs. (17) and (19)-(21) can be rewritten in the form

$$\begin{aligned}
xu'_i &= x^2 f_i , & i &= 1 - 3 , \\
xv'_i &= -\lambda_i v_i + x^2 g_i , & i &= 1 - 4 ,
\end{aligned} \tag{69}$$

where f_i and g_i are analytical functions of x^2 , u_j , v_j and $1/N$ and $\lambda_i = 3$, $i = 1, 2, 3$. It now follows from Proposition 1 of Appendix A of [5] that the system of equations (17) and (19)-(21) admits a three-parameter family of solutions of the form

$$u_i = c_i + O(x^2) , \quad v_i = O(x^2) \tag{70}$$

which are locally analytic in x^2 and in the constants c_i . These constants correspond to h_1 , j_1 and k_2 in (64).

7.2 Appendix A.2

Following [8] and considering the system of equations (27)-(35), we here demonstrate the local existence of the non-abelian dyonic black hole solutions at the singular point x_h . Black hole solutions are characterized by a first order pole singularity of the function κ at the non-degenerate horizon [8]. Due to translation invariance of the equations under $\tau \rightarrow \tau + \tau_0$, we can assume that the horizon occurs at $\tau = 0$.

To rewrite the set of equations in the form (69), which reveals the number of free parameters occurring in the expansion at the horizon of the locally analytic solution, we introduce the following set of functions

$$\begin{aligned}
(u_1, u_2, u_3, u_4, u_5) &= (r, W, H, 2\kappa N - 2U^2 - V^2, S) , \\
(v_1, v_2, v_3, v_4) &= (\kappa - \frac{1}{\tau}, U, V, Y - S(\kappa - \frac{1}{\tau})) ,
\end{aligned} \tag{71}$$

with

$$S = B/\tau , \quad Y = \dot{S} . \tag{72}$$

These functions are regular at the horizon and can be expanded in powers of τ . Moreover, it follows that the equations for u_i and v_k are of the form (69) with $\lambda_1 = 2$, $\lambda_2 = \lambda_3 = 1$ and $\lambda_4 = 3$. This demonstrates the existence of a five-parameter family of local analytic solutions of the equations. Because of the constraint (36), it actually reduces to a four-parameter family of local solutions.

Figure Captions

Figure 1

The normalized mass of the regular dyon solutions is shown as a function of the charge Q for vanishing Higgs self-coupling ($\beta = 0$) and finite Higgs self-coupling ($\beta^2 = 0.5$) for the flat space solutions (solid lines) and curved space solutions with $\alpha = 0.5$ (dashed lines). The asterisks mark the transition from exponentially decaying solutions to oscillating solutions.

Figure 2

Same as Fig. 1 for the asymptotic value of the function $J(x)$.

Figure 3

The mass of the solutions of the 1st excited dyon branch for $Q = 1$ and the 1st excited monopole branch ($Q = 0$) is shown as a function of the coupling constant α for $\beta = 0$ (solid). Also shown is the mass of the branch of extremal RN solutions with unit magnetic charge and $Q = 1$ as well as $Q = 0$ (dotted). The normalization is chosen such that at $\alpha = 0$ the mass of the first Bartnik-McKinnon solution is obtained.

Figure 4

The domain of existence of the dyonic black hole solutions in the $\alpha - x_h$ plane is shown for $Q = 1$. The straight diagonal line represents the extremal RN solutions. To the right of this line only non-abelian black hole solutions exist. Here the limiting curve represents the maximal values of α , while the second curve close to it represents the critical values of α , where the solutions bifurcate with the corresponding extremal RN solution. The asterisk marks the critical value $\hat{\alpha}$. To the left of the line of extremal RN solutions both non-extremal RN solutions and non-abelian black hole solutions coexist below the upper curve, representing the maximal horizon radius as a function of α . The small rectangle indicates the critical region, where bifurcations occur (enlarged in Fig. 10). Below the bifurcations, the lower curve represents the critical values of the horizon, where the solutions terminate because $J_\infty = 1$ is reached.

Figure 5

The quantities DN , DK , DP and DH are shown as functions of the parameter α for the dyonic black hole solutions with $Q = 1$ and $x_h = 0.8$. The second branch of solutions in the interval $1.1986 \leq \alpha \leq 1.2002$ is clearly visible.

Figure 6

The functions $N(x)$ and $P(x)$ are shown for the dyonic black hole solutions with $Q = 1$ and $\alpha = 1$ for the horizon radii $x_h = 1, 1.1$ and 1.153 .

Figure 7

Same as Fig. 6 for the functions $K(x)$ and $H(x)$.

Figure 8

The quantities DN , DK , DP and DH are shown as functions of the horizon radius x_h for the dyonic black hole solutions with $Q = 1$ and $\alpha = 0.94 > \hat{\alpha}$.

Figure 9

Same as Fig. 8 for $\alpha = 0.93 < \hat{\alpha}$.

Figure 10

Enlargement of the critical region (small rectangle) of Fig. 4, showing the domain of existence of the dyonic black hole solutions in the $\alpha - x_h$ plane for $Q = 1$. The numbers 0-3 indicate the numbers of solutions in the respective areas. A and C indicate the critical values, where the bifurcations occur, D indicates the critical value, where the transition from the limiting non-extremal RN solutions to the oscillating solutions occurs. $J_\infty = 1$ is reached along the curve $A'ABD$.

Figure 11

The quantities $K(x_h)$, $H(x_h)$ and J_∞ are shown as functions of the horizon radius x_h for the dyonic black hole solutions with $Q = 1$ and $\alpha = 0.7$.

Figure 12

Same as Fig. 11 for $\alpha = 0.55$.

Figure 13

Same as Fig. 11 for $\alpha = 0.2$.

Figure 14

The charge Q , corresponding to the critical value D , where the transition from the limiting non-extremal RN solutions to the oscillating solutions occurs, is shown as a function of α (dotted). Also shown is the critical value $\hat{\alpha}$ (solid).

Figure 15

The minimum of the function $N(x)$ is shown as a function of the parameter α for the first radially excited dyonic black hole solutions with $Q = 1$ and horizon radii $x_h = 0.01, 0.4$ and 0.8 .

Figure 16

The functions $N(x)$, $P(x)$, $K(x)$ and $H(x)$ are shown for the first radially excited dyonic black hole solution with $Q = 1$, $\alpha = 0.938$ and $x_h = 0.4$.

Fig. 1

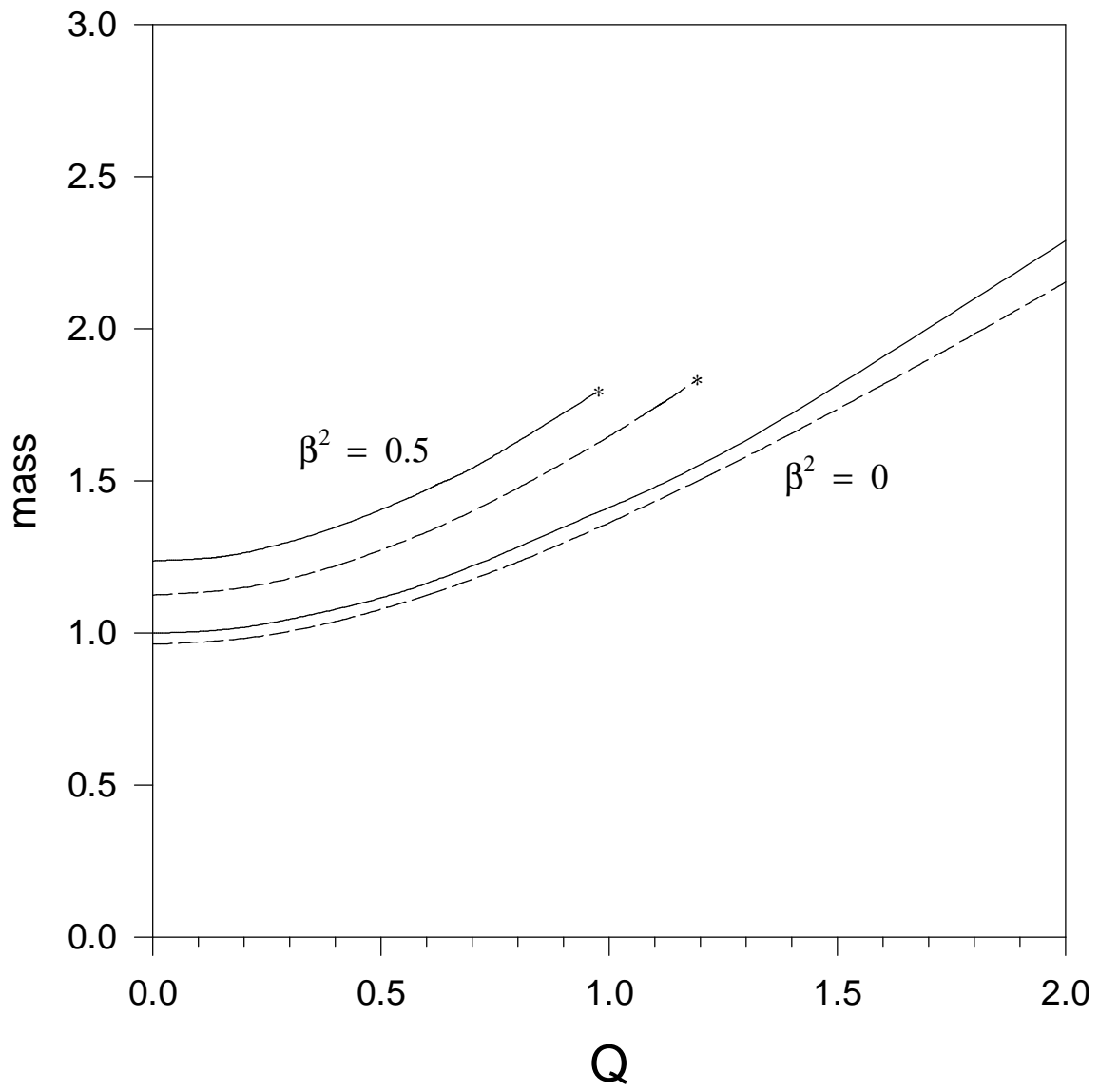


Fig. 2

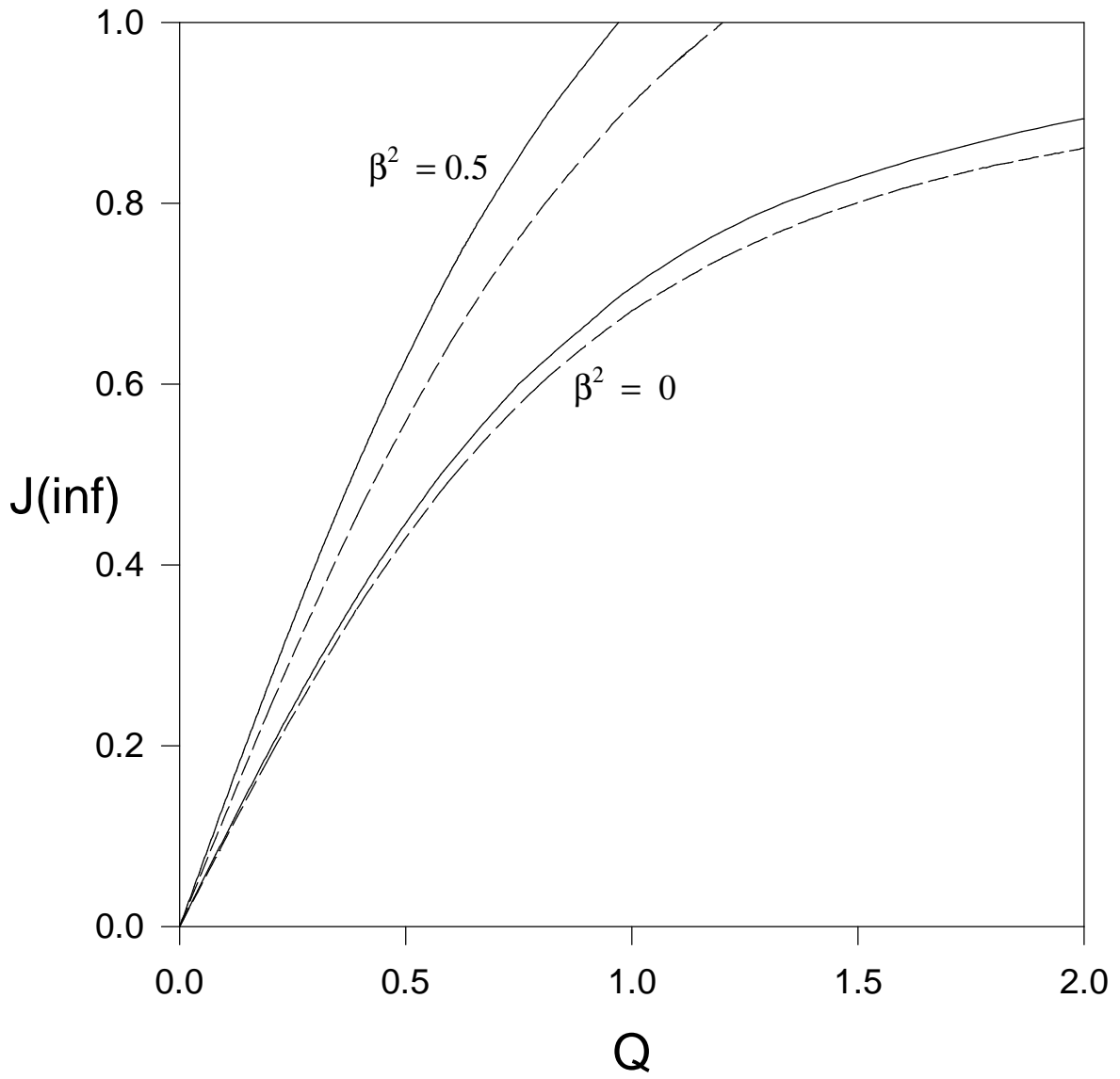


Fig. 3

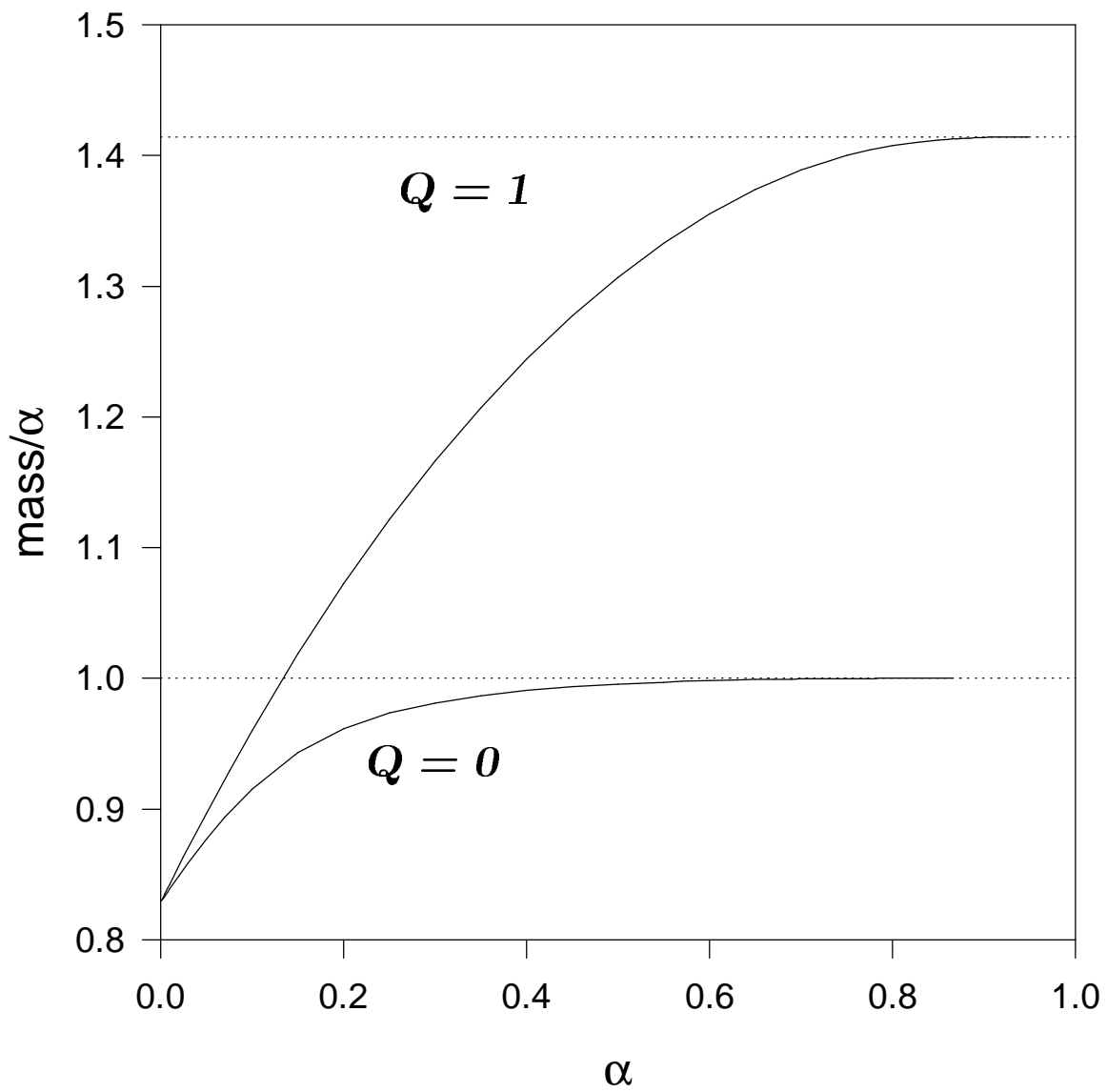


Fig. 4

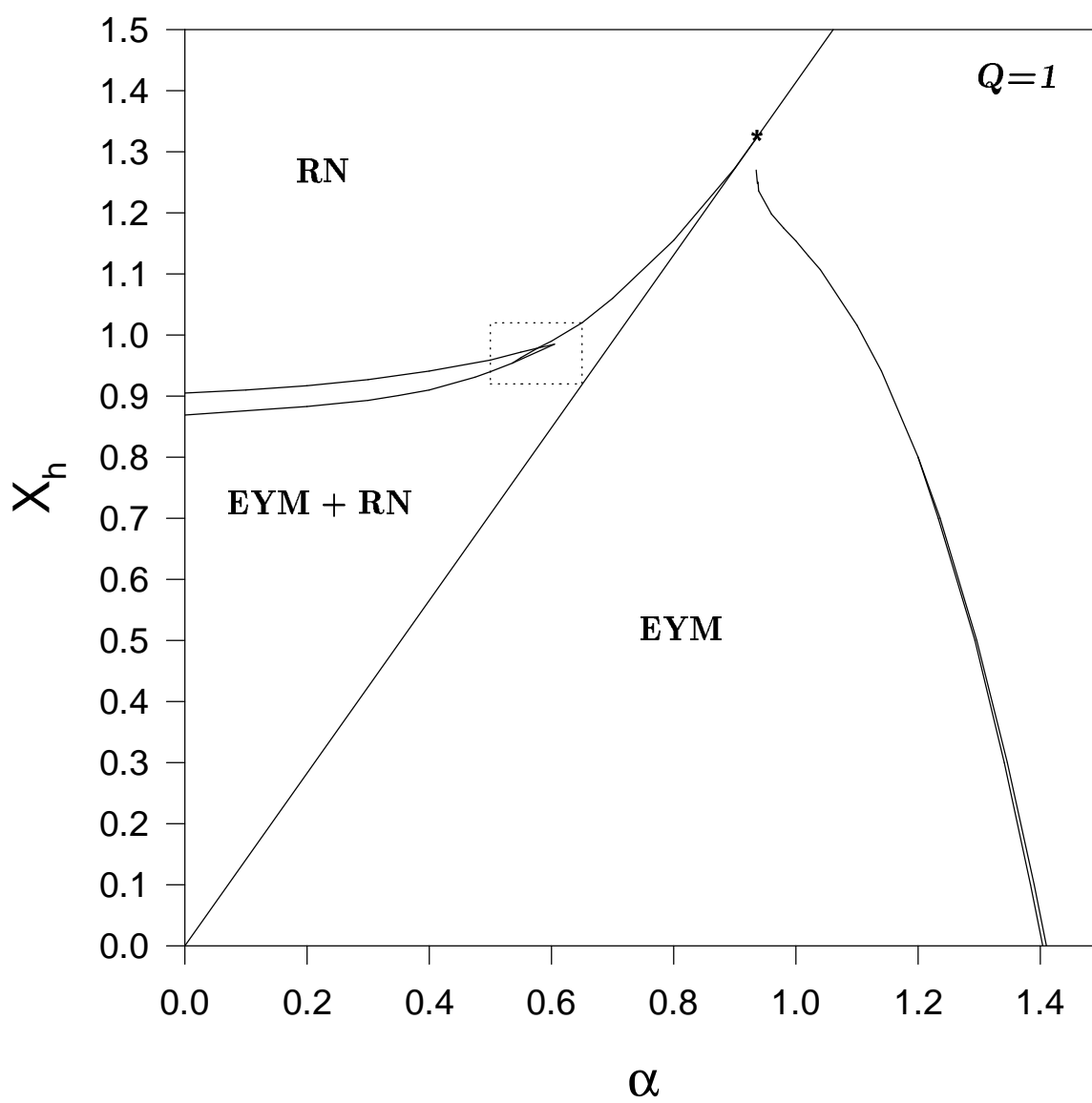


Fig. 5

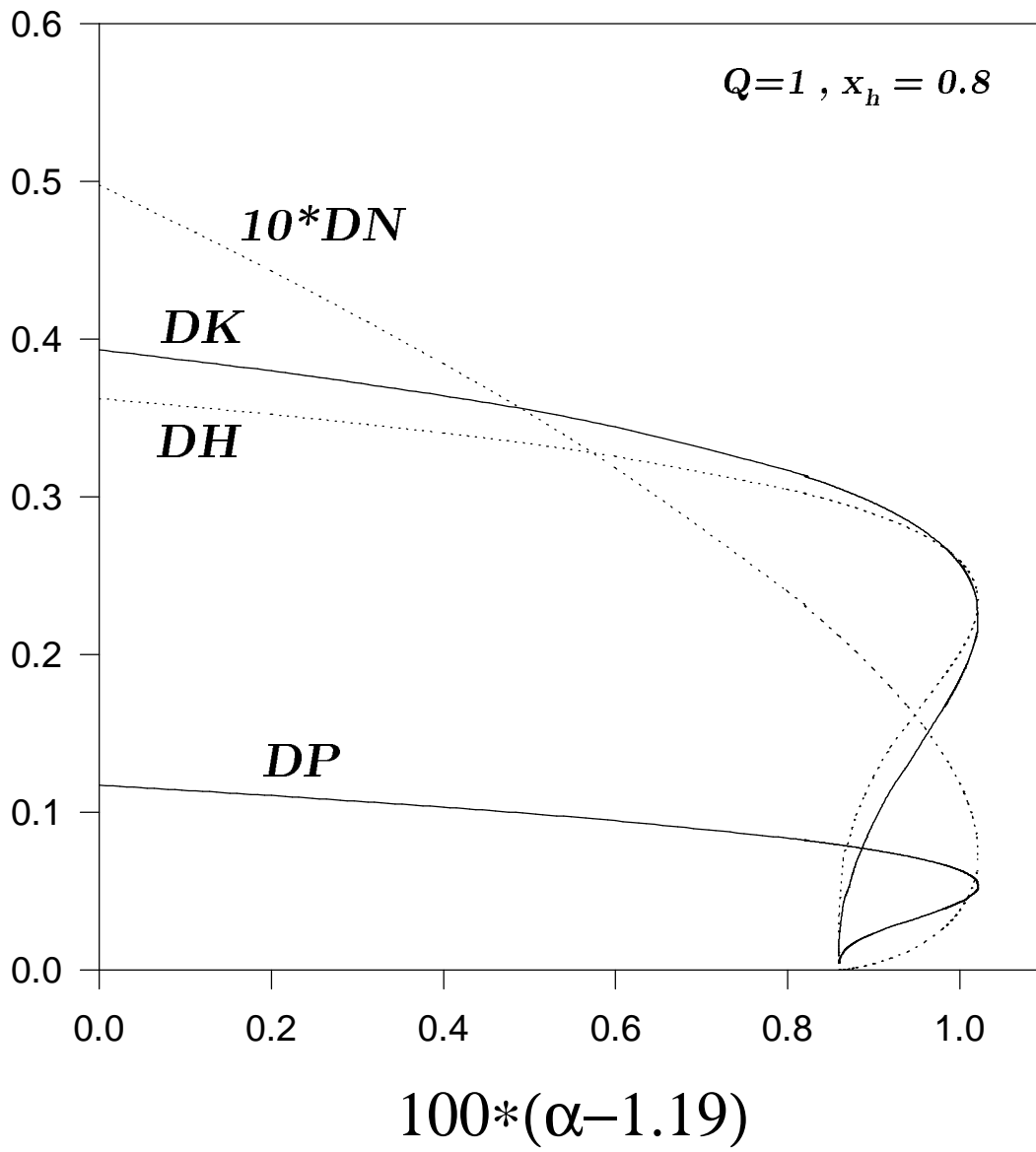


Fig. 6

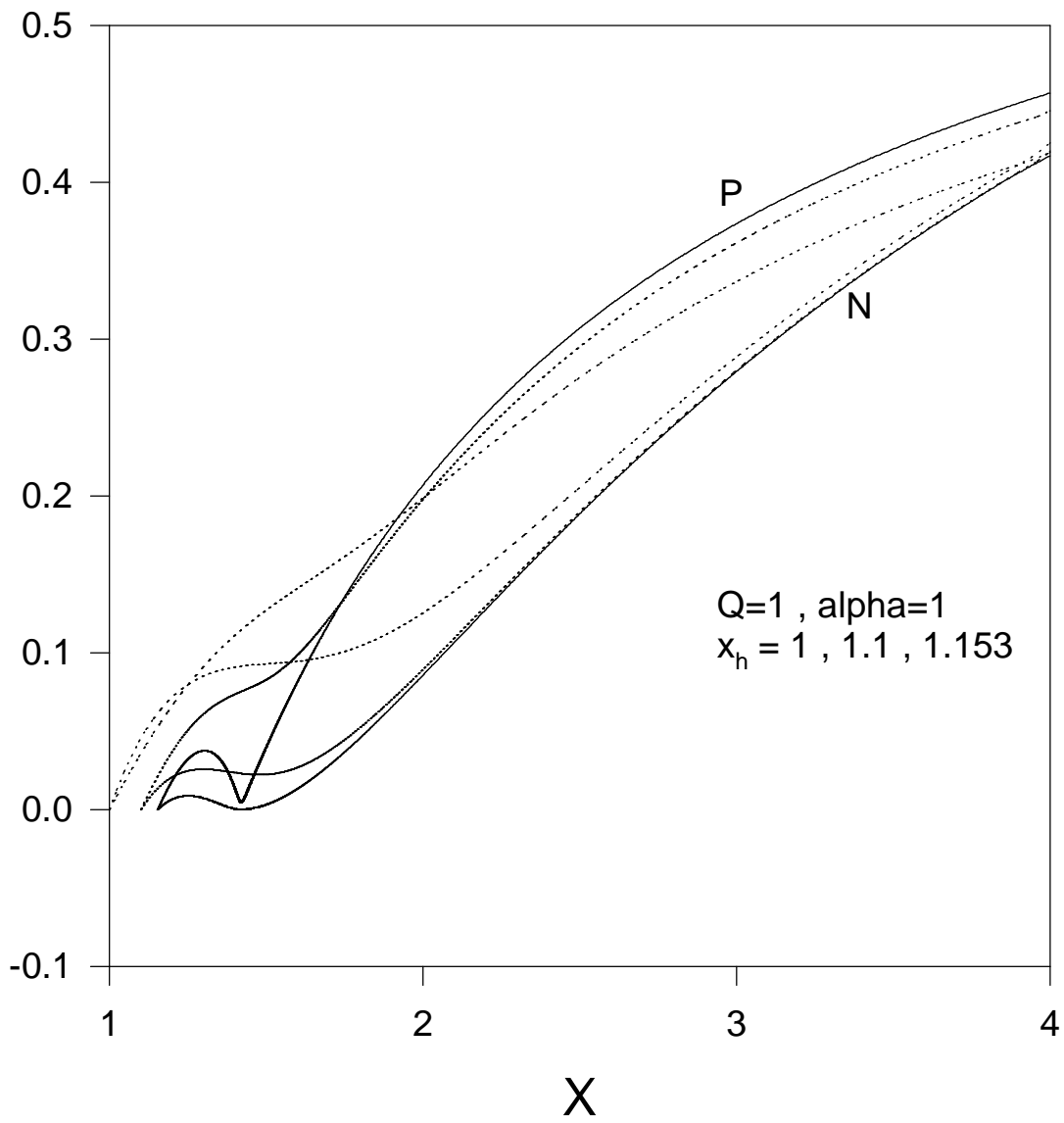


Fig. 7

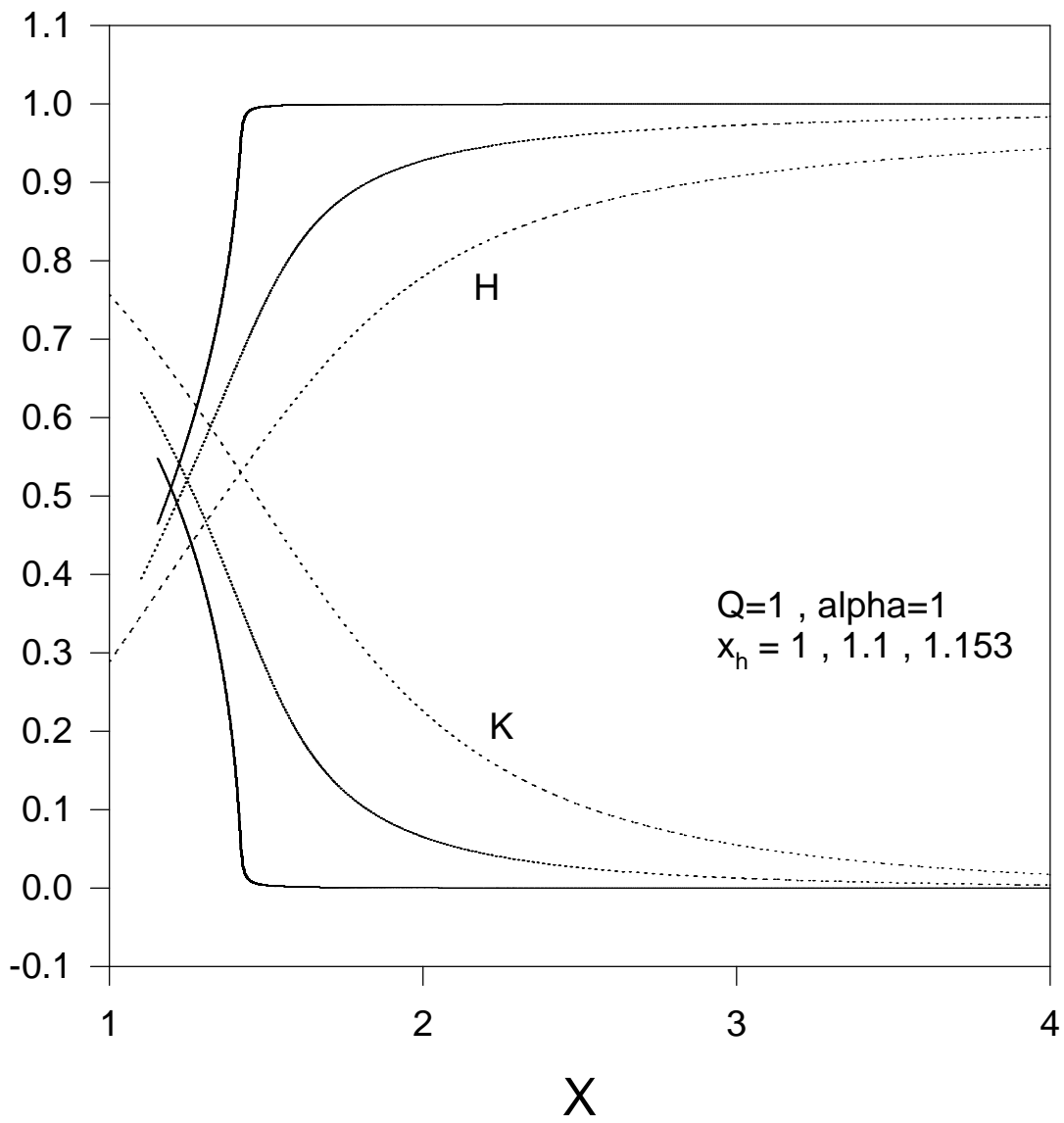


Fig. 8

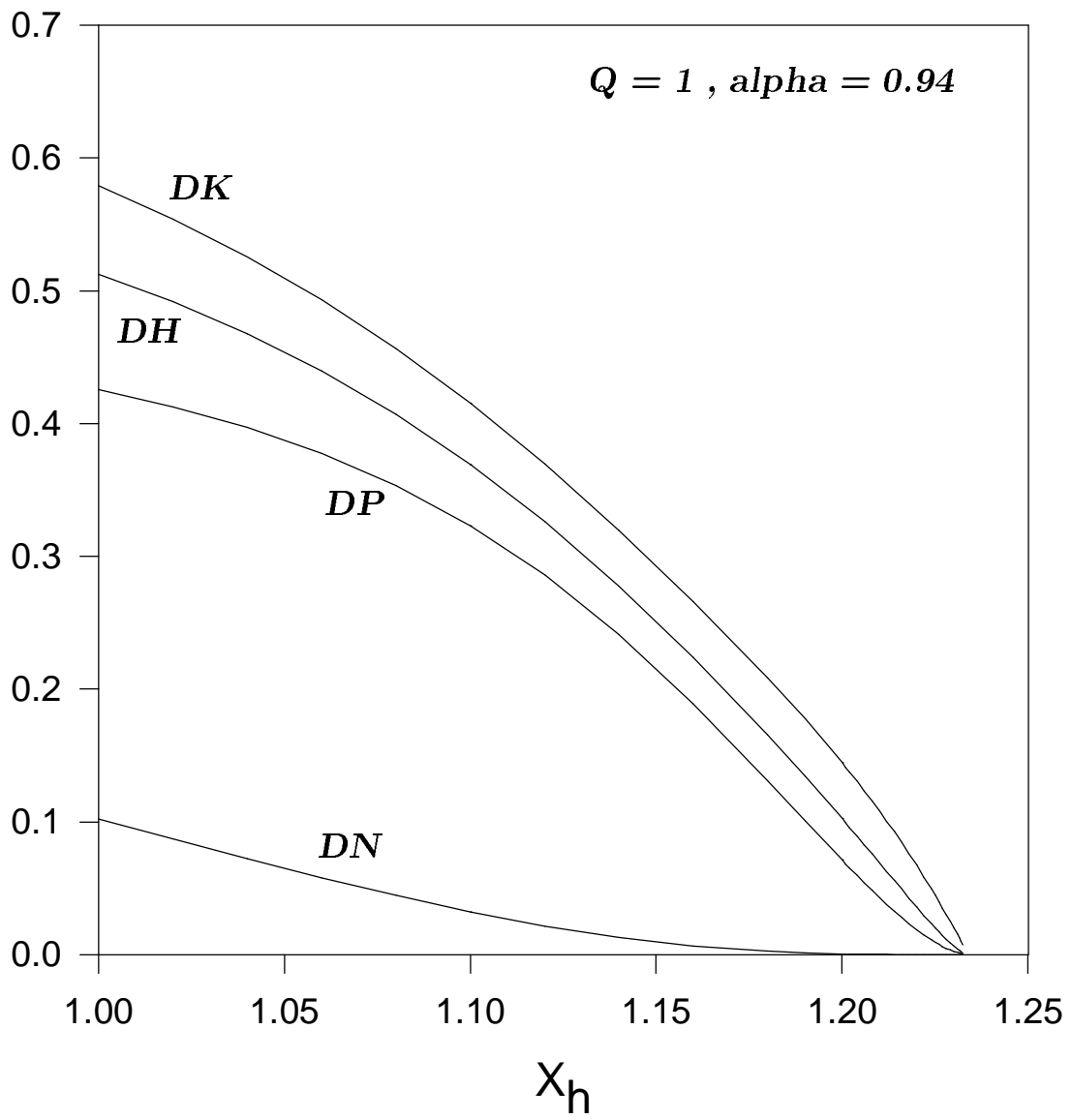


Fig. 9

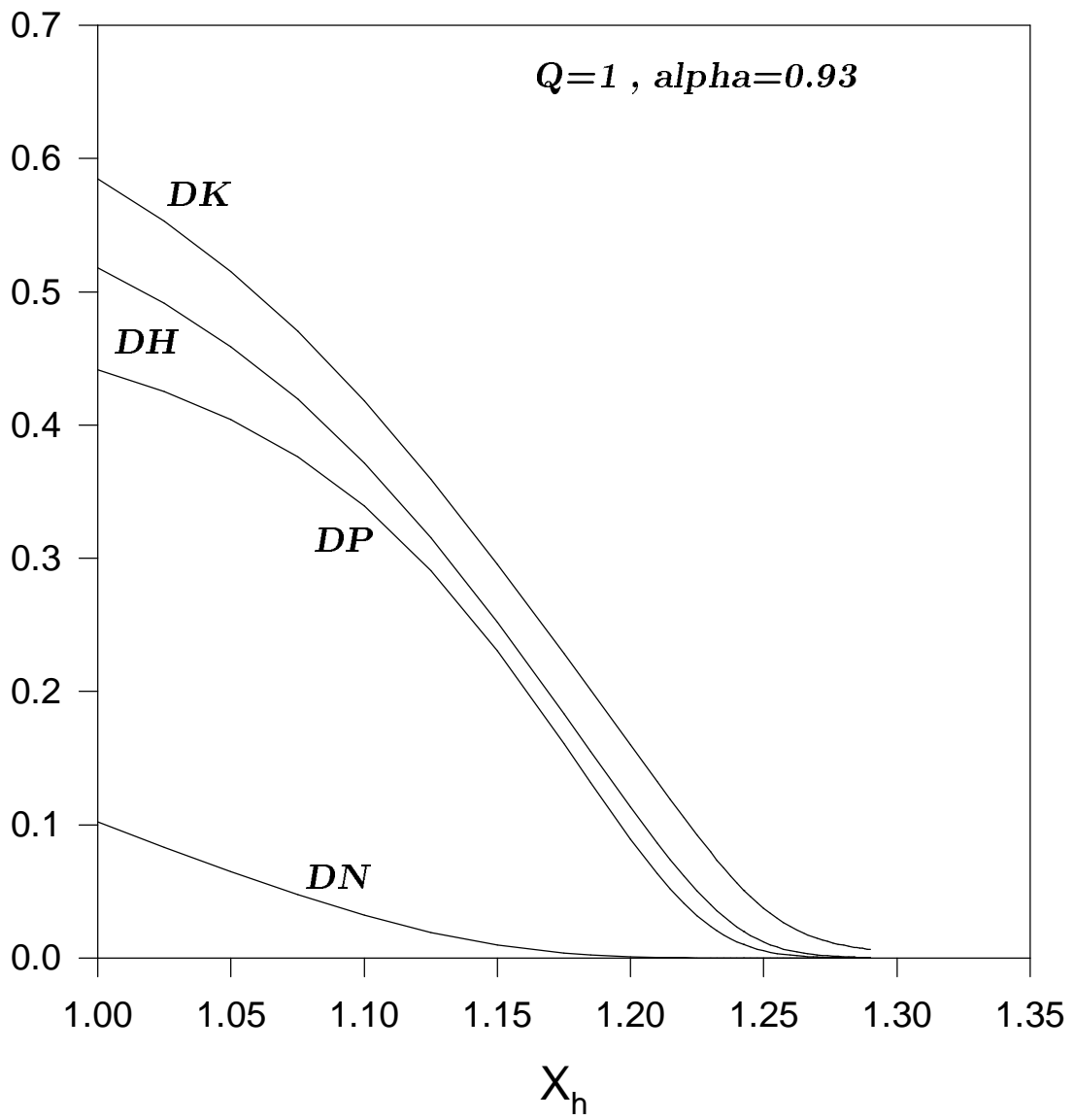


Fig. 10

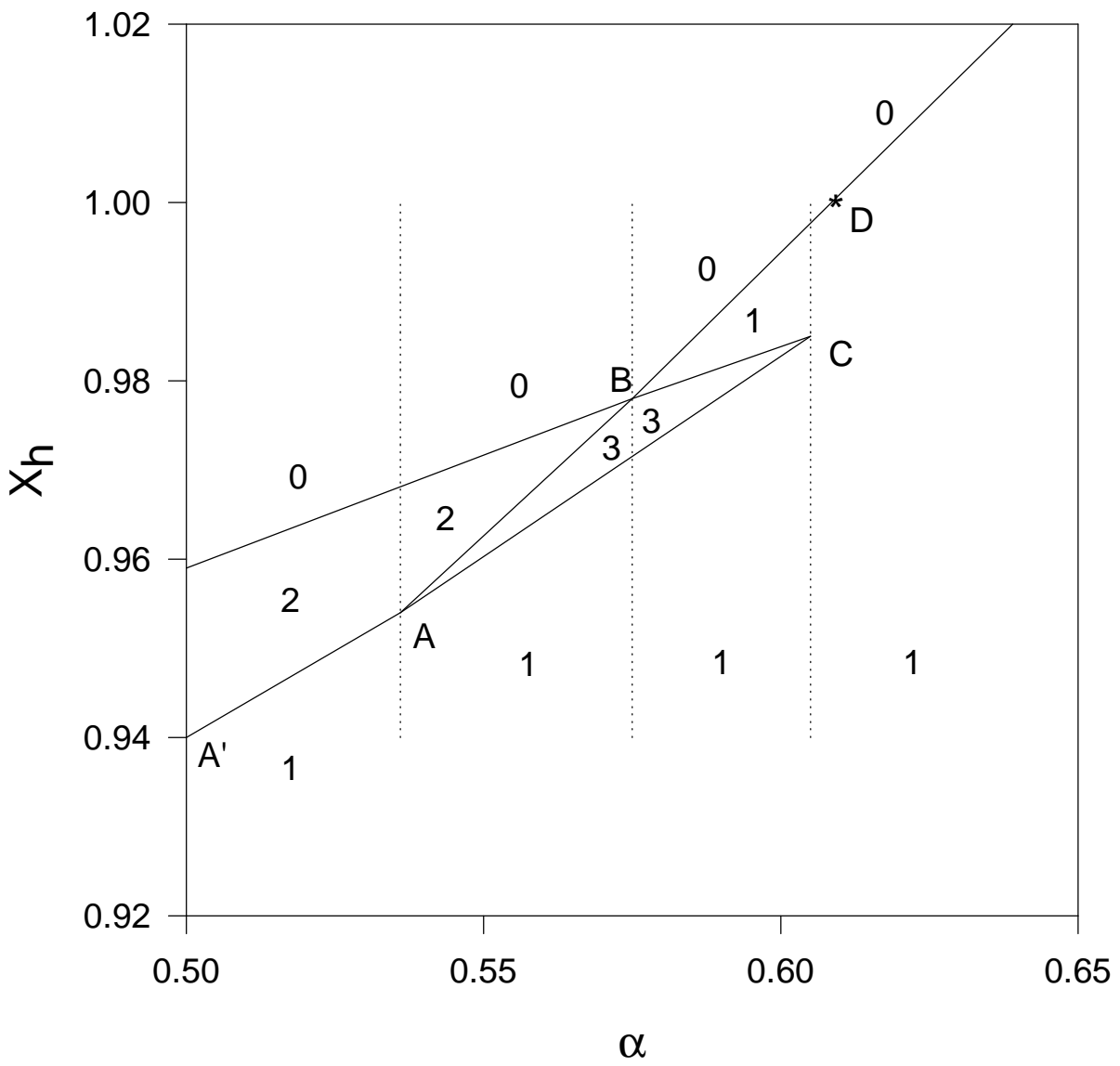


Fig. 11

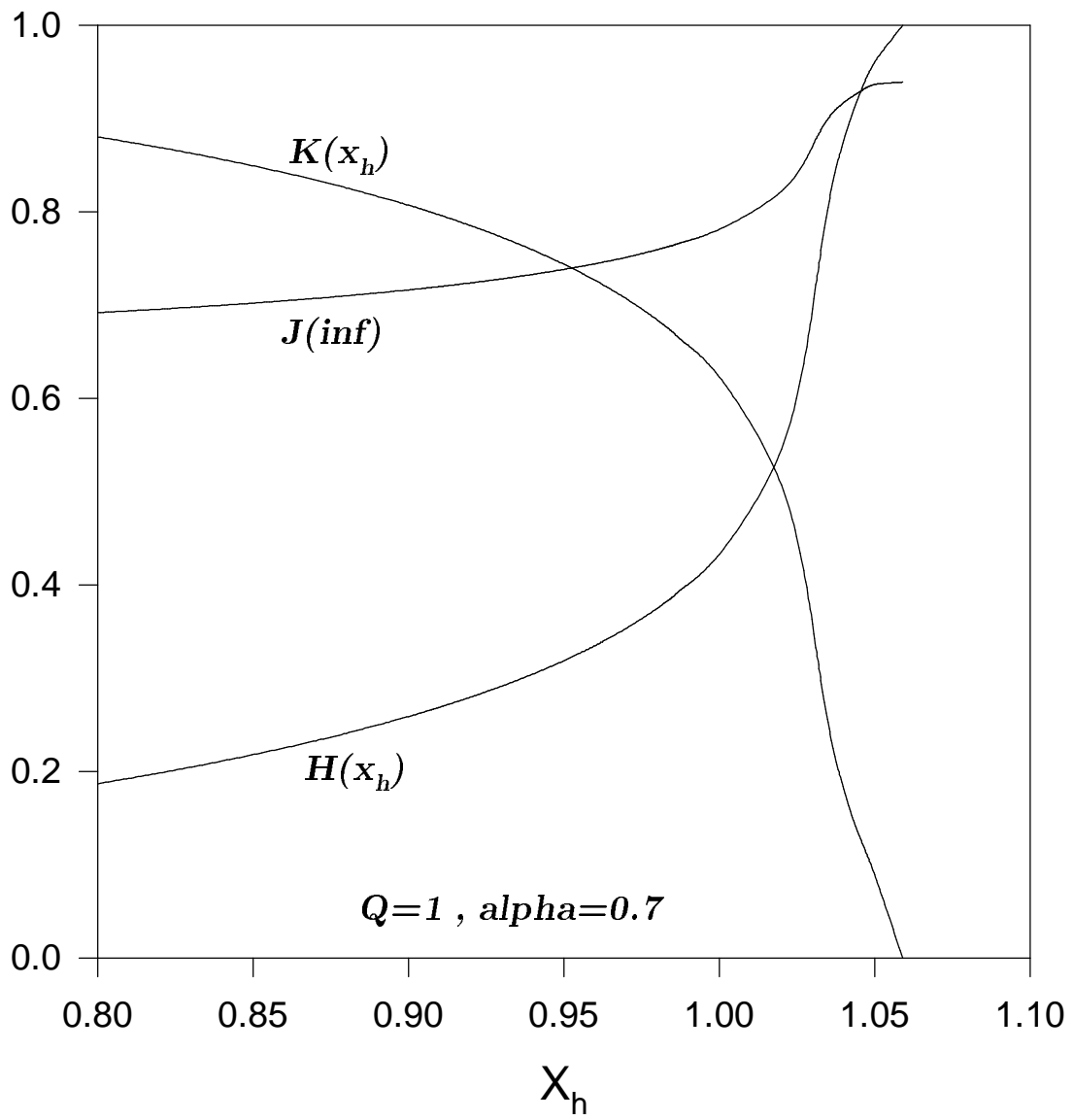


Fig. 12

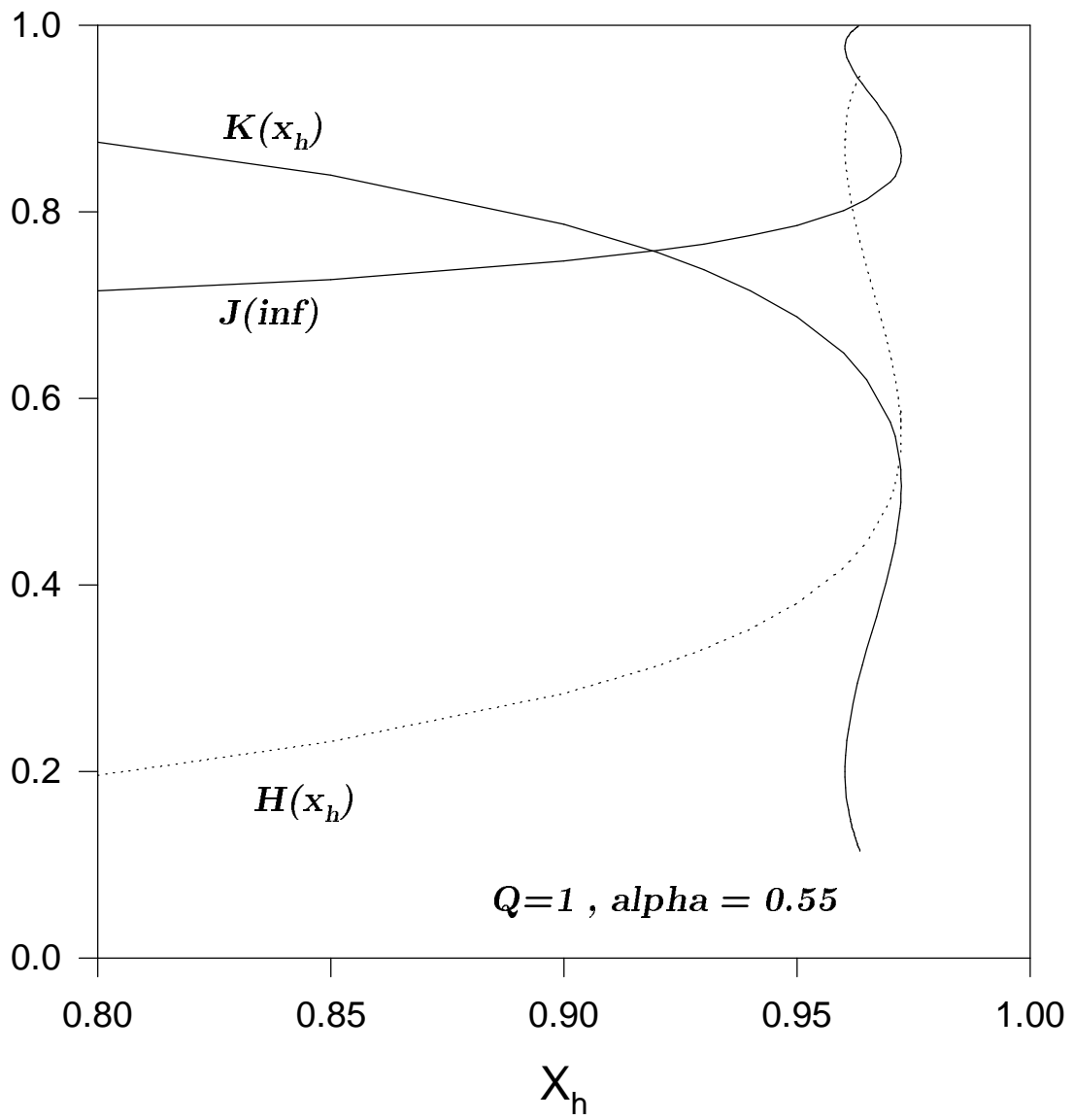


Fig. 13

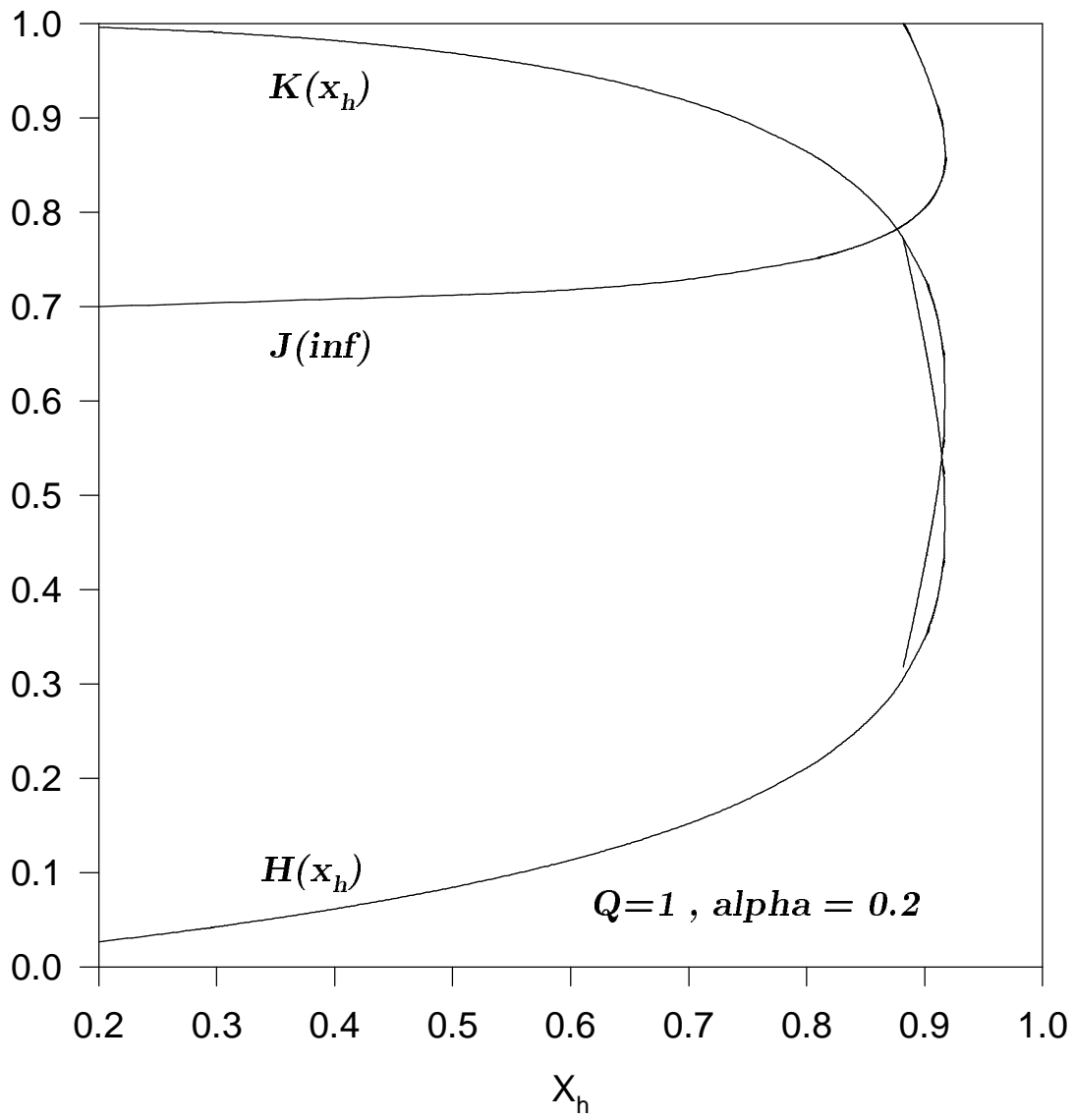


Fig. 14

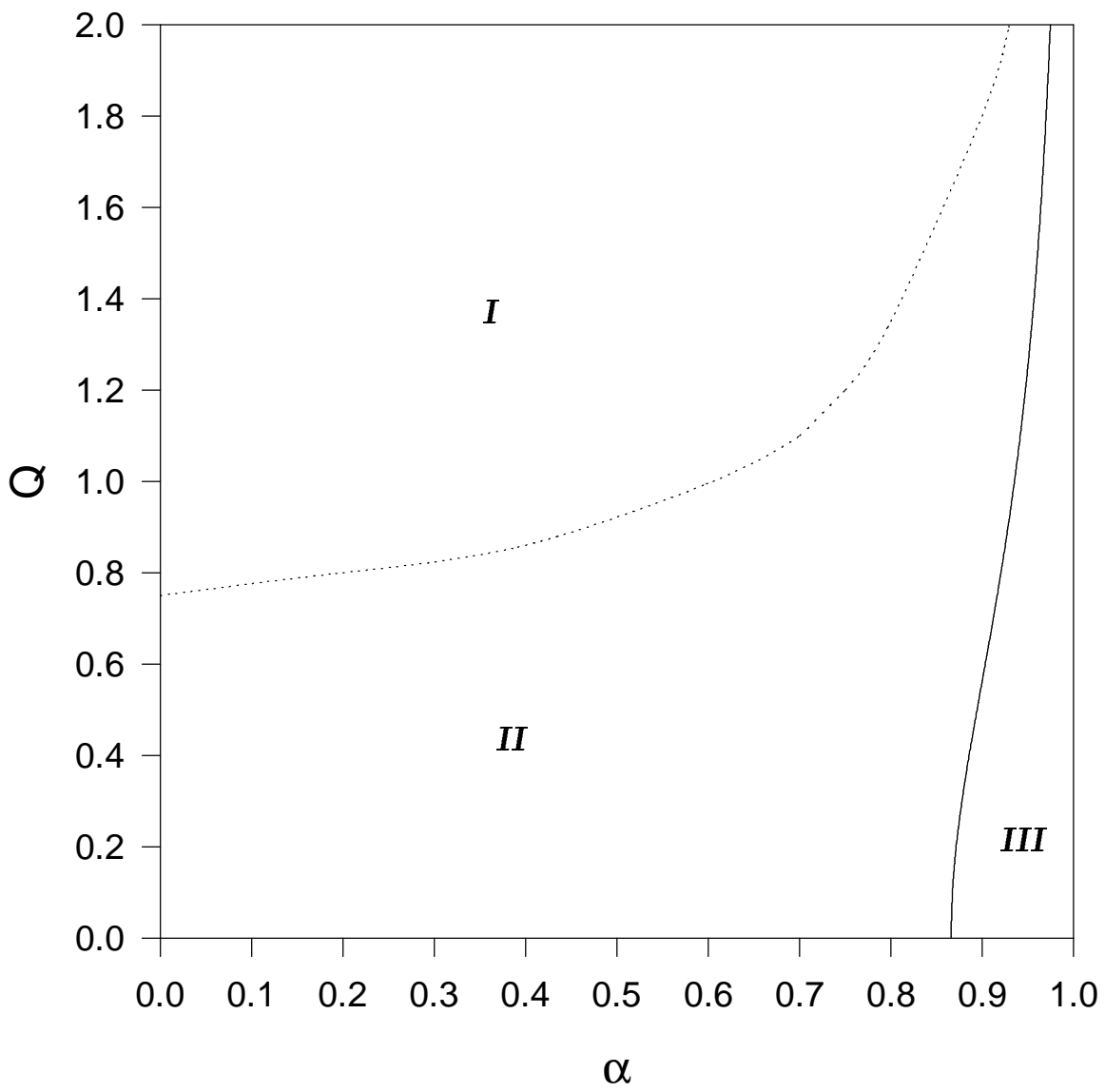


Fig. 15

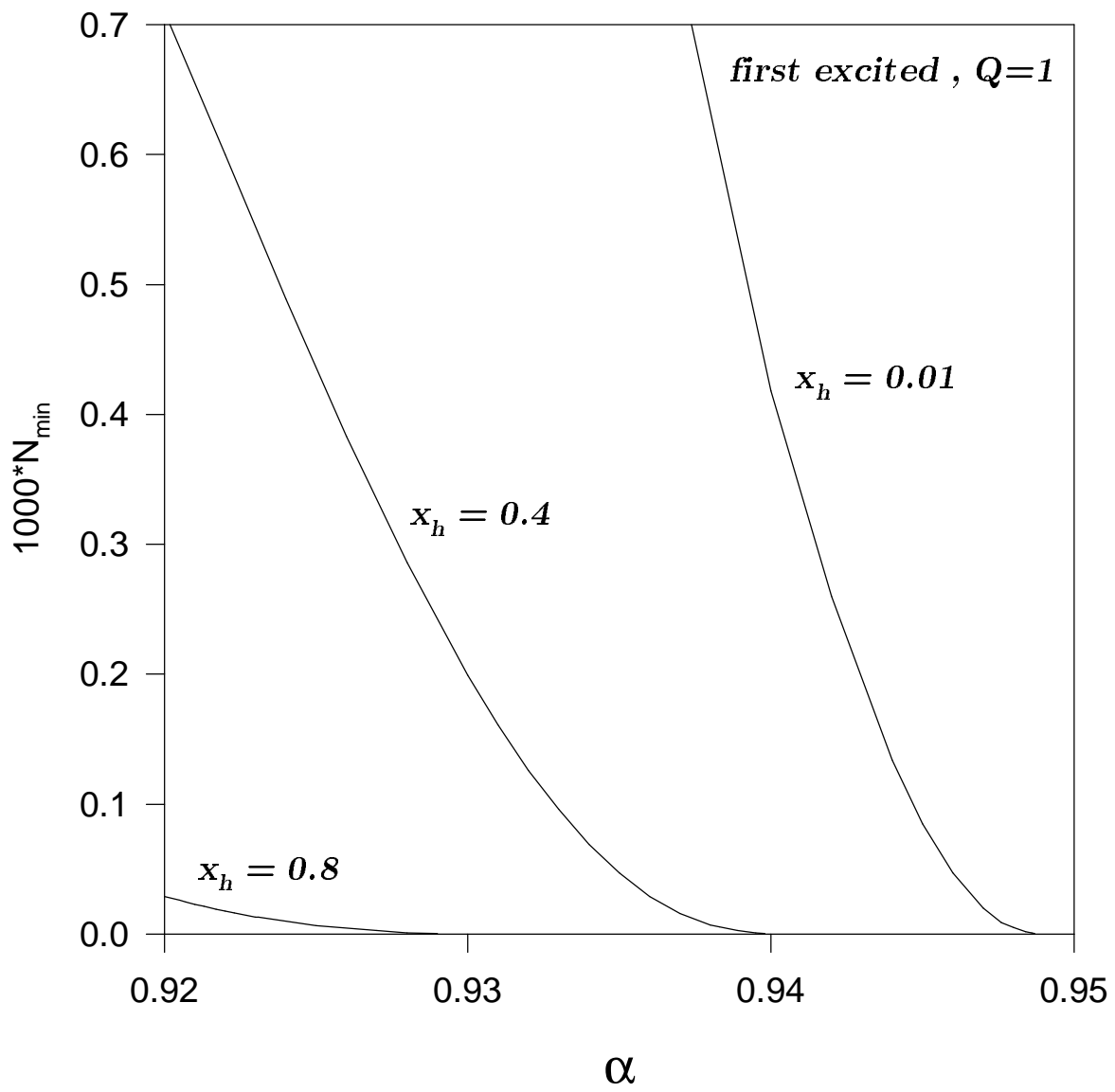


Fig. 16

